SPIQ-FS Dataset

Version 0

Adjustments to SPIQ-FS marginal damage cost models to estimate damages in future scenarios

Steven Lord

Environmental Change Institute, University of Oxford

Content reviewer:

Citation: Lord, S. (2022) Adjustments to SPIQ-FS marginal damage cost models to estimate damages in future scenarios. Documentation of the SPIQ-FS Dataset Version 0. Environmental Change Institute, University of Oxford.

Environmental Change Institute

eci

UNIVERSITY OF OXFORD

FoodSIVI

Summary

The original SPIQ-FS dataset provided marginal damage costs in US$2020 PPP for GHG emissions, nitrogen emissions to air and surface waters, land-use changes, etc. occurring in the baseline year of 2020 [1-5]. This document examines the adjustments to the SPIQ-FS model required to provide a time series of marginal damage costs in US$2020 PPP for activities (emissions, etc.) occurring in 2020, marginal damage costs in US$2030 PPP for activities occurring in 2030, marginal damage costs in US$2040 PPP for activities occurring in 2040, and marginal damage costs in US$2050 PPP for activities occurring in 2050, under scenarios of future economic conditions. The decadal time steps are nominal, but 2050 is chosen as the ceiling for the adjustments.

To adjust the costs, economic scenarios need to be specified as a time series of socio-economic and demographic projections at national level, such as Gross Domestic Product (GDP PPP) growth [6, 7], Human Development Index (HDI) [8], population changes, labour participation, age dependency, urban rural ratio, Gross National Income per capita estimated by the Atlas method (GNI Atlas) [9], and trends in national total non-communicable disease rates such as cardio-vascular disease, type II diabetes, and neoplasms [10]. Many of these variables are correlated, and projections based on vector autoregression methods are advocated [11]. Table 2 provides a table of the economic and demographic variables suggested to adjust marginal damage costs.

Given the economic and demographic variables in Table 2, some damage cost adjustments are straightforward. An example is inflating GDP damages by the GDP growth factor. Most cost models, and most common modules, within SPIQ-FS use the economic and demographic variables, alongside other variables, within linear and non-linear regressions derived from historical data. These relationships have been examined in SPIQ-FS to reduce the number of variables, to reduce the potential for correlation effects between the variables, and for explanatory power. Including the economic and demographic variable in the SPIQ model regressions affords non-linear adjustments to damages given projection of the economic and demographic variables.

For example, disability adjusted life years (DALYs) per capita from protein-energy malnutrition historically fit a quadratic function of prevalence of undernutrition (PoU) and HDI. The two factors of PoU and HDI explain 70% of the variance amongst countries, and the 30% that is unexplained by more complicated differences in national healthcare, dietary intake, disease burdens, and social supports, etc. is reflected in modelled uncertainty in the damage costs. Models such as the International Food Policy Research Institute's (IFPRI's) MIRAGRODEP computable general equilibrium model [12] can estimate changes in PoU, which, alongside a projection of HDI, and another module of SPIQ-FS which sets the cost to GDP of a DALY, affords a projection of the damage costs from future changes in DALYs from protein-energy malnutrition.

The design of the SPIQ-FS model, and the examination of relationships such as the one described in the previous paragraph, provides the means to adjust the damage costs estimates. Subsequent sections examine each component of the SPIQ-FS model for adjustment. Dependence on the economic and demographic variables in Table 2 is described, and relevant internal adjustments to the 2020 model components discussed.

The conclusion of the examination is that there are achievable changes to the SPIQ-FS model that can provide adjustment to marginal damage costs for future scenarios, provided that: (a) those scenarios can be translated into time series projections of the economic and demographic dimensions listed in Table 2, and (b) the interaction of the scenarios with internal modelling components can be specified.

Contents

Acknowledgements:

The author thanks Food System Economic Commissioners Simon Dietz (LSE) and Rachel Nugent (RTI International) for discussions on relative pricing of ecosystem services and economic costs attributable to dietary intake.

1 Adjustments to the SPIQ-FS model for temporal projections

1.1 Components of the SPIQ-FS model

The SPIQ-FS version 0 has model components for damage costs for four environmental outcomes from food system activities and, as of version 0.1, has model components for three health outcomes from dietary intake [1-5].

The environmental components calculate marginal damage costs with uncertainty for quantities of greenhouse gas (GHG) emissions, reactive nitrogen pollution to air and surface waters, withdrawal of blue water, and land-use changes, that are attributable to food system activities [13-16]. The uncertainty is modelled for each component along the pathway from the emission, withdrawal, or land-use change to the economic impact [17, 18].

The health components calculate marginal damage costs for changes in body mass index (BMI), for the burden of non-communicable disease (NCD) resulting from dietary intake, and for undernourishment. Again, with explicit uncertainty modelling.

Some SPIQ-FS model components are based on open-source existing models, such as the cost of GHG emissions model is based on the IWG-SCGHG simulations of the social cost of carbon [19, 20], and the BMI and NCD costs factor through reconstructions of the respective University of Washington Global Burden of Disease models [21, 22]. Other components have been developed specifically within SPIQ-FS. These details are documented in Annex A of the SPIQ-FS documentation [1-5].

SPIQ also has common modules that are shared between the cost models. This is to ensure consistency. One such model is a GDP projection module for discounting impacts in years after the emission or pollution activity [23, 24]. It ensures a social discount rate, [25], is applied consistently within the same 'economic future' in all cost models . Another is a module for costing DALYs [26], which is used for costing air pollution effects from nitrogen pollution [27], malnutrition effects from blue water withdrawal [28], and disease burden from food consumption [16, 21].

1.2 Economic, development, and demographic factors

The SPIQ-FS improves, reworks, or directly uses, already published models to estimate marginal damage costs. A set of marginal damage costs m is the estimate of the additional cost (as measured by GDP loss) to a country c for a unit increase to one element of a vector of quantities q in the context of a vector of economic and demographic factors [29, 30]:

$$m(c, q, e).$$

The quantities, units, and definition of damages can be found in the SPIQ-FS documentation of version 0. SPIQ-FS is for large scale economic modelling, and it is used to generate a dataset that contains $m(c, q, e)$ for >160 countries and >10 quantities to be coupled with other economic modelling that determines the relevant unit increases in the quantities q for those countries. The quantity changes q from some baseline q_0, as determined by that other economic modelling, estimates the decrease or increase in damages $I(c)$ for a country c by

$$I(c) \coloneqq m(c, q, e) \cdot q - m(c, q_0, e_0) \cdot q_0 .$$

It is generally assumed that the economic and demographic factors e for the country c remain fixed, or that the changes are sufficiently small such that $m(c, q, e) \cong m(c, q, e_0)$. Constant "shadow prices" are also often assumed, meaning that the quantity changes q-q_0 are sufficiently small, or the damage costs are so inelastic to the quantity change q-q_0, that the approximation $m(c, q, e) \cong m(c, q_0, e_0)$ is valid.

Studies of the change in damages over decades, where the economic and demographic factors of countries are likely to change [31], and where it is unclear that damage costs are inelastic to quantity changes over such a time span [32], require that the marginal damage costs be specified for quantities and economic conditions covering the range of expected changes [33]. That is, for such studies, the assumption of constant marginal damage costs loses validity [34, 35].

Studies consider the changes over time under different versions of the future, called scenarios [32, 36]. These different versions of the future may or may not specify different food systems or societal actions. Such distinctions are not relevant for the present argument, other than that we wish to estimate damage costs not only for a country c with present economic and demographic factors e_0 (such as GDP, population, HDI, etc.) and quantities q_0 at the present time. The indexing required for considering national damage costs in plausible futures is (c, s, t), where $e(c, s, t)$ denotes a projection of the economic and demographic factors of a country c at a time t in the future under the scenario s. Similarly, $q(c, s, t)$ denotes the quantities of GHG emissions, or nitrogen emissions, etc. of a country c at a time t in the future under the scenario s.

The vectors $e(c, s, t)$ and $q(c, s, t)$ may be jointly dependent. It is often the case in partial equilibrium economic modelling that the data $e(c, s, t)$ is used to set exogenous components for the endogenous calculation of $q(c, s, t)$, [37, 38]. In computable general equilibrium modelling, the economic and demographic data may be framed as constraints or determined endogenously with quantities through simultaneous and lag relationships [39, 40]. The coupling of $e(c, s, t)$ and $q(c, s, t)$ as projections of e and q into the future under alternative scenarios is determined by a prior modelling step and is external to the SPIQ-FS model.

We assume that the vectors $e(c, s, t)$ and $q(c, s, t)$ are determined and given.

Coupling between the historical economic and demographic data and the historical level of quantities has been included in the SPIQ-FS modelling, within the functions $m(c, q, e)$. Additional adjustments, as described below, project forward changes in couplings deemed required as adjustments to the functions $m(c, q, e)$.

Subsequent sections document adjusting the SPIQ-FS model to obtain estimates of marginal damage costs in future scenarios, that is vectors

$$m\big(c, q(c, s, t), e(c, s, t)\big)$$

for a country c at a time t in the future under the scenario s. The damages

$$\begin{aligned} I\big((c_1, s_1, t_1), (c_0, s_0, t_0)\big) \\ \coloneqq\; & m\big(c_1\,, q(c_1, s_1, t_1), e(c_1, s_1, t_1)\big) \cdot q(c_1, s_1, t_1) \\ -\; & m\big(c_0\,, q(c_0, s_0, t_0), e(c_0, s_0, t_0)\big) \cdot q(c_0, s_0, t_0) \end{aligned}$$

therefore allow a comparison for a fixed country ($c_1 = c_0$) or set of countries over time in the same scenario ($s_1 = s_0$), or a comparison for a fixed country ($c_1 = c_0$) or set of countries at the same time ($t_1 = t_0$) for different scenario.

1.2.1 Specification of economic, development, and demographic factors for SPIQ-FS

This section describes the economic, development and demographic dimensions used in the adjusted SPIQ-FS model. The time series $t \mapsto e(c, s, t)$ for each country c and each scenario s for the dimensions in Table 1 need to be provided so that the adjusted SPIQ-FS model can calculate a set of marginal damage costs.

Table 1: Tabular format of the economic, development and demographic variables used in the adjusted SPIQ-FS model. Each country, scenario, and time, triplet is specified values of the variables described in Table 2. The format is illustrated for two countries (A,B) under 3 scenarios (1,2,3) with 3 time steps (2020,2030,2050).

Country (*c*)	Scenario (*s*)	Time (*t*)	Economic, developmental, demographic variables (*e*)												
			GDP PPP	HDI	GNI	Pop	Lab Trend	EMUC	WPPA	WDFA	FPPI	Age Dep	URR	ERP	ATemp
A	1	2020	*	*	*	*	*	*	*	*	*	*	*	*	*
A	1	2030	*	*	*	*	*	*	*	*	*	*	*	*	*
A	1	2050	*	*	*	*	*	*	*	*	*	*	*	*	*
A	2	2020	*	*	*	*	*	*	*	*	*	*	*	*	*
A	2	2030	*	*	*	*	*	*	*	*	*	*	*	*	*
A	2	2050	*	*	*	*	*	*	*	*	*	*	*	*	*
A	3	2020	*	*	*	*	*	*	*	*	*	*	*	*	*
A	3	2030	*	*	*	*	*	*	*	*	*	*	*	*	*
A	3	2050	*	*	*	*	*	*	*	*	*	*	*	*	*
B	1	2020	*	*	*	*	*	*	*	*	*	*	*	*	*
B	1	2030	*	*	*	*	*	*	*	*	*	*	*	*	*
B	1	2050	*	*	*	*	*	*	*	*	*	*	*	*	*
B	2	2020	*	*	*	*	*	*	*	*	*	*	*	*	*
B	2	2030	*	*	*	*	*	*	*	*	*	*	*	*	*
B	2	2050	*	*	*	*	*	*	*	*	*	*	*	*	*
B	3	2020	*	*	*	*	*	*	*	*	*	*	*	*	*
B	3	2030	*	*	*	*	*	*	*	*	*	*	*	*	*
B	3	2050	*	*	*	*	*	*	*	*	*	*	*	*	*

Table 2: Economic, development and demographic variables used in the adjusted SPIQ-FS model. Links describe the variable methodology and sources historical data series.

Variable	Description
GDP PPP	Gross Domestic Product (GDP) projection of country c in scenario s in international dollars in year t (GDP in year t in local currency exchanged to US dollars in year t and adjusted for purchasing power parity in year t) https://data.worldbank.org/indicator/NY.GDP.MKTP.PP.CD
HDI	Human Development Index of a country c in scenario s at time t. The human development index is a relative scale in [0,1], with 1 indicating the high level of development at time t. https://hdr.undp.org/data-center/human-development-index#/indicies/HDI
GNI	Gross National Income per capita (GNI) for country c in scenario s at year t determined by the World Bank Atlas method (not adjusted for PPP). https://data.worldbank.org/indicator/NY.GNP.PCAP.CD
Pop	Population (headcount of individuals) projection of country c in scenario s at time t. https://www.un.org/development/desa/pd/content/World-Population-Prospects-2022
LabTrend	The change in the ratio of labourers per capita for country c in scenario s at year t. Index with base value 1 corresponding to the ILO estimate of the labourers per capita for country c in year 2020. https://ilostat.ilo.org/data/
EMUC	Elasticity of the marginal utility of consumption (EMUC). Optional specification of EMUC for country c in scenario s for inter-temporal comparison of damages using social discount

	rates. https://www.jstor.org/stable/24440019
WPAA	Water Productivity Agricultural Adjustment for country c in scenario s at time t. A proportion index estimating increases in volume of food supply (as a proxy for both caloric and value increase) from same water supply and same real costs of production. Baseline is 1 in 2020. Due to the large proportion of freshwater consumed by the agricultural sector in crop production, water efficiency indicators are defined by water productivity in agriculture https://www.sdg6data.org/indicator/6.4.1
WDFA	Water Deprivation Factor Adjustment for country c in scenario s at time t. A proportion index estimating increases in economic output across all sectors from the same water supply. Baseline is 1 in 2020. https://ec.europa.eu/eurostat/web/products-datasets/-/t2020_rd210
FPPI	Food Producer Price Index (FPPI) projection of country c in scenario s at time t with base year the FAO Producer Price Index 2020. FPPI is the increase or decrease in farm gate prices averaged across commodities. http://fenix.fao.org/faostat/internal/en/#data/PP
AgeDep	World Bank age dependency ratio is the ratio of dependents--people younger than 15 or older than 64--to the working-age population--those ages 15-64. Data are shown as the proportion of dependents per 100 working-age population. https://data.worldbank.org/indicator/SP.POP.DPND
Urban Rural Ratio (URR)	World Bank urban population refers to percentage of people living in urban areas as defined by national statistical offices. The data are collected and smoothed by United Nations Population Division. https://data.worldbank.org/indicator/SP.URB.TOTL.IN.ZS
ERP	Relative growth in pricing of ecosystem services compared to general consumption growth. Combination of changes in the marginal value of ecosystem services due to the pricing of natural capital flows by the economy (demand), technological advances in the efficiency of using natural capital, and reduced supply from environmental damage or increased supply from reversing environmental damage. https://www.pbl.nl/en/publications/relative-price-increase-for-nature-and-ecosystem-services
ATemp	National mean temperature increase in degrees Celsius of a country c in scenario s at time t. Base value is 0 when year t is 2020. https://climateknowledgeportal.worldbank.org/download-data

The time variable t should be between 2020 and 2050. Validity of historically trained regressions in SPIQ-FS would be expected to get significantly weaker with increased uncertainty for time spans outside 2050. Since impacts for food system activities in 2050 continue to occur for decades [13], or centuries in the case of GHG [41], discounting the future damages creates additional uncertainty [42, 43]. The default recommendation is that discounting rates be specified for 2020-2100 for activities in the period 2020-2050. Projections are available up to 2100. Time spans beyond 2050 would push the need to project GDP growth for individual countries beyond 2100.

1.2.2 Coding the economic, development, and demographic factors into SPIQ-FS

A SPIQ-FS build means that the SPIQ-FS model is run to create a dataset of marginal damage costs $m\big(c, q(c,s,t), e(c,s,t)\big)$ indexed by (c,s,t). The time series $t \mapsto e(c,s,t)$ for each country c and each scenario s as in Table 1 are represented for a SPIQ-FS build in a build file. The original SPIQ-FS build, or build 0, described in Annex A, is indexed by (c,s,t) where $t = 2020$ and the single scenario s is the baseline "the world as was at the start of 2020".

The scenarios s specified by a particular study, and which are encoded in the build file, are hereafter referred to as build scenarios.

The build file contains a structure. One of the elements of the structure is a table containing the values $e(c,s,t)$ of the economic and demographic parameters for each country to be studied at each time step and for each build scenario (Table 1). That is, the table contains the time series projections of the economic and demographic variables of last section for each country under each build scenario. One build generates the marginal costs for all countries, all time steps, and all scenarios specified in the structure.

The build structure contains other variables determined by the build scenarios that are used internally in the costing models. As an example, the GHG costing model uses IGW-SCGHG simulations [19, 20]. The social cost of carbon simulations conducted by IGW-SCGHG used 5 scenarios to explore future uncertainty in economic activity. A weighting matrix is used to describe similarity of a build scenario, at a particular time, to the IGW-SCGHG simulation scenarios used for simulations of the social cost of carbon. The weights can change for each time step, reflecting that the similarity of the build scenarios to the IGW-SCGHG simulations scenarios can change over time.

1.3 Adjustment to SPIQ-FS model components

Annex A contains the full documentation of chosen components, modelling results, analysis of uncertainty, and caveats for the SPIQ version 0 models [1-5]. Here we stylise the components of each model as a schematic and depict their interaction with: (a) the quantities q such as GHG emissions that are determined by a given study and (b) the economic and demographic factors e of build scenarios, discussed in Section 1.2 and outlined in Table 2. We also discuss internal model adjustments, such as the use of a weighting matrix as described in the preceding paragraph.

We start with the common modules and then move to the environmental and health costing models.

1.3.1 Module 101: growth projections for discounting and inflating

Module 101 specifies GDP growth projections g from 2020-2100 for each year for each country c in each scenario s. GDP is measures in purchasing power parity (PPP) [7]. The projections are used to downscale global GDP projections and must be fully consistent, or used to construct, the GDP variable in the data $e(c, s, t)$ provided.

SPIQ uses the growth projections for finer resolution inflation and discounting of future damages in the water, land-use, and air pollution costing models. In the GHG cost model, the growth projections are also used to match build scenarios as closely as possible to the IGW-SCGHG simulations of the social cost of carbon in the GHG cost model [19, 20]. The IGW-SCGHG provides simulations for a range of discounting rates (2.5%, 3%, and 5%) [19]. The growth rates specified in module 101 are matched as closely as possible in a build file to the corresponding IGW-SCGHG interest rate.

As fundamental economic data, the country level and annual GDP growth times series can support filling in time series of other economic variables in Table 1 using vector autoregression type models trained on historical relationships [11].

SPIQ default GDP growth projections for 2020-2100 use future GDP growth projections for the 5 Shared Socioeconomic Pathways (SSPs) over the periods 2020-2040 and 2040-2100 from Table 3 in [24]. [24] uses its own division of countries into high, medium, and low income as of 2020 with different projections for each group. Countries are assigned the GDP projections for their income groups.

Default builds of SPIQ that do not specify future scenarios use [24] and sample randomly from the 5 SSPs to simulate uncertainty in future GDP growth. It is recommended that the scenarios s in custom builds be specified so that they represent a range of potential future GDP growth trajectories, and future uncertainty in GDP growth represented by the build scenarios be used rather than the random sampling of adjusted projections from [24].

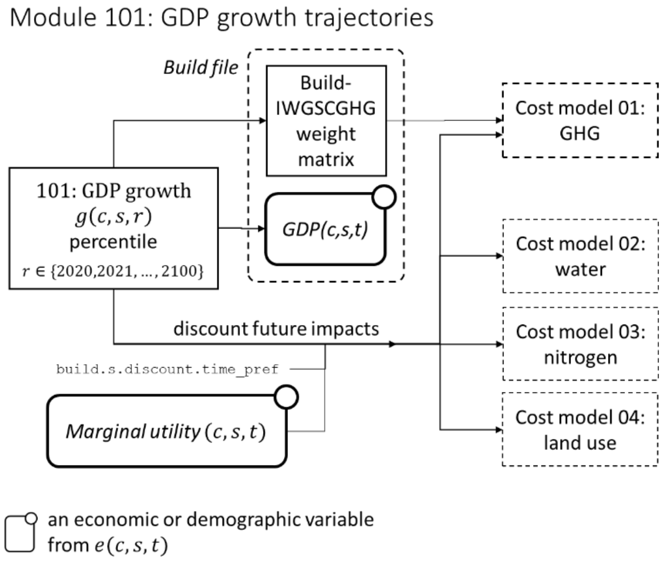

Figure 1: GDP growth rates for countries and scenarios. Other settings in a build file can be used to set the social discount rate for discounting future damages.

When GDP growth trajectories are used for discounting, the default discount rate is treated as a Ramsey social discount rate (SDR) with time preference of 0 and in with constant elasticity of marginal utility of 1. These settings can be adjusted for custom builds. The time preference can be set to a global value in a SPIQ build file, and the elasticity of marginal utility can be separately set for each country and each scenario as an economic parameter (EMUC in Table 2) [44]. The literature on SDR is extensive [25, 45], but it is recommended to use a conservative value for intergenerational wealth transfer given current wealth generation from food system activities may be endogenous to the risk of the ability to enjoy deferred resource use [46-48]. The potential volatility of future welfare accrual and the nature of consumption as a proxy for welfare in a future with environmental and health damages, means that lower settings for the elasticity of marginal utility are recommended [49-51].

Consistency between module 101 and the GDP variable in Table 1, necessitates the constraints

$$GDP(c,s,t) = \prod_{r \leq t} \big(1 + g(c,s,r)\big) \cdot GDP(c,s,2020).$$

1.3.2 Module 102: cost of DALYs

This module costs disability-adjusted life years (DALYs) [52-54] and is used for costing air pollution effects on humans from nitrogen pollution [55], malnutrition effects from blue water withdrawal [28], and disease burden from poor or insufficient diets [56-58].

As explained in Annex A SPIQ-FS documentation, DALYs arise from multiple disease outcomes and disease pathways, including but not limited to cardiovascular disease from air particulate matter [59], diabetes type II from diets high in sugar and low in whole grains [60], neoplasms from diets low in nutrients and high in red and processed meats [61], and protein-energy malnutrition [62]. The module intends to cost the economic burden to society due from premature death and the effects of disablement for each disease outcome and disease pathway [56, 57, 63].

Since the marginal costs need to be consistent across costing models, the cost from DALYs focus only on so-called indirect costs on income equivalent welfare [64]. Direct costs amount to economic exchanges between sectors and actors within the economy, [65], and are not included since there are few estimates of the inefficiency of the direct costs flowing to the health sector from individuals or government. Income equivalent welfare treats the population homogeneously, so it does not include potential welfare losses from direct costs being borne disproportionately by lower income households.

Version 0 of the SPIQ model costs a DALY in a country by productivity loss [66], and it is simplified as the same amount irrespective of the disease outcomes or the disease pathway. More details and considerations are in Annex A [5]. Later versions of SPIQ-FS will consider productivity losses from DALYs for different outcomes, starting with primary categorical divisions into cardiovascular disease, type II diabetes, and neoplasms, [67].

The cost of a DALY in country c in scenario s is in GDP PPP in the year t.

The build file which contains the output of module 102 contains 3 cost values for each index (c, s, t).

$CF_1(c, s, t)$ uses on the global average value of labour productivity as projected from 2017 ILO data (https://ilostat.ilo.org/data/). Each country has the same value.

$CF_3(c, s, t)$ uses on the national average value of labour productivity as projected from 2017 ILO data. Each country has a different value, and the difference between countries can be up to 2 orders of magnitude in PPP terms.

$CF_2(c, s, t)$ uses the average value of labour productivity within World Bank income brackets (low income, low-middle income, middle-high income, high income) as projected from 2017 ILO data. Each country is assigned the value of its income bracket as time t in scenario s.

Advantages and disadvantages for using any of the 3 values are discussed in Annex A [5]. By default, following [67], a SPIQ-FS build uses CF_2 values.

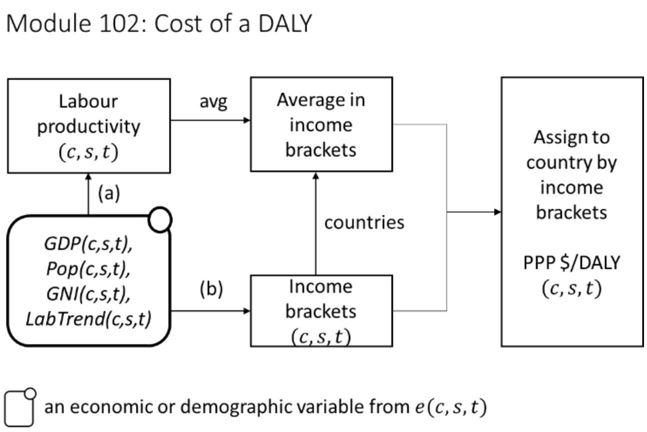

Figure 2: (a) Labour productivity is calculated from labour productivity from ILO 2017 data for country c inflated using historical GDP growth to 2020. The value $LabProd(c, 0{,}2020)$, is inflated by future GDP growth and altered by the projection in labourers:

$$LabProd(c, s, t) = LabProd(c, 0{,}2020) \cdot \frac{GDP(c, s, t)}{GDP(c, 0{,}2020)} \cdot \frac{Pop(c, 0{,}2020)}{Pop(c, s, t) \cdot LabTrend(c, s, t)}$$

(b) Criteria for belonging to income at time t depends on GNI of country c in scenario s at time t. The income brackets themselves, i.e. their upper and lower thresholds at time t, are projected from WB historical shifts in thresholds. The labour productivity is averaged within projected income brackets, and a PPP \$/DALY cost assigned according to the income bracket a country c belongs to at time t in the scenario s. Figure shows calculation of the output CF_2 value. Other outputs follow the same calculation, with an adjustment to the 'income brackets' being either world (one bracket) in the case of CF_1, or individual countries as 'brackets' in the case of CF_3.

The formula for projected forward labour productivity is written in such a way as to use relative growth or trend instead of absolute values. GDP growth, population growth, and the growth or deflation in the labourers per capita are used to calculate future labour productivity from present data [68].

1.3.3 Module 103: DALYs per capita from undernourishment

This module calculates the change in DALYs per capita due to protein-energy malnutrition given a change in the prevalence of undernourishment [62, 69], for the country c at a time t in the future under the scenario s. It is based on a robust truncated quadratic relationship between historical DALYS per capita due to protein-energy malnutrition from World Health Organization (WHO) historical data [70], prevalence of undernourishment (PoU) measured by the UN Food and Agriculture Organization (FAO), and HDI as calculated by United Nations Development Programme (UNDP). HDI is a primary explanatory factor for when undernutrition in a population translates into preventable disease and death [69]. Bayesian regression is used [71], meaning that a probability family of quadratic relationships is determined from historical data to account for variance not explained by PoU and HDI. The partial derivative with respect to PoU of the (family of) quadratic surface(s) results in a relationship between change in DALYs and change in PoU that depends on HDI.

HDI has more explanatory power in the regression than GNI or GDP. More detail can be found in Annex A [3].

Heteroskedasticity in the errors over different HDI ranges means that the uncertainty is also modelled with dependence on HDI. The relationship is robust to data from historical years before the present. The Bayesian quadratic regression is used to project forward the random variable of change in DALYs per capita due to protein-energy malnutrition given a change in the prevalence of undernourishment by using the HDI for the country c at a time t under the scenario s.

The output of module 103 can be considered as the uncertain numbers of DALYs per person undernourished in country c in scenario s in the year t.

Module 103 is used in the water costing model as part of the malnutrition cost component, and it is used in the costing of undernourishment model. Module 103 has a second variant, that is based on a similar regression between DALYs from protein-energy malnutrition involving PoUW, prevalence of underweight persons (BMI < 18.5 [72, 73]), instead of PoU. The output of the variant can be considered as the numbers of DALYs per person underweight in country c in scenario s in the year t.

Using only protein-energy malnutrition DALYs may undercount attributable all outcomes DALYs from prevalence of undernourishment and underweight in the population [74]. Module 103 is used in costing model 02 where changes in undernourishment are due to reduction in domestic food supply, where protein-energy malnutrition may be expected to be the predominant outcome. Use of the PoUW variant of Module 103 should be considered in the context of the drivers of change in PoUW. In adults in developed countries, the drivers of underweight prevalence are more diverse than food supply and food prices, and protein-energy malnutrition as a disease outcome is expected to capture proportionally less of the population outcomes from underweight prevalence [75].

Module 103: DALYs per capita from undernourishment

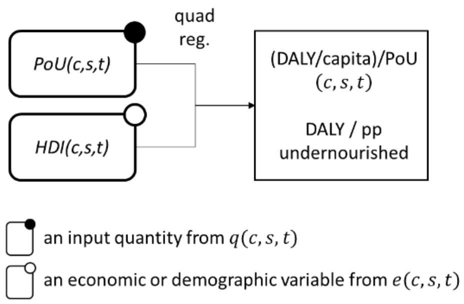

Figure 3: The partial derivative of protein-energy DALYs per against PoU in a Bayesian quadratic regression allows the DALYs per person undernourished to be treated as a random variable and projected forward using HDI.

1.3.4 Module 104: ecosystem service values

This module calculates ecosystem service values based on statistical analysis of the Ecosystem Service Valuation Database (ESVD) [76, 78].

Despite the database having nearly 3000 useable valuations of ecosystem services for 49 ecosystem categories and 23 service categories, the database does not have sufficient statistical coverage of countries, ecosystems, and services to use directly. ESVD uses the TEEB Classification and CICES (v5.1) classification systems of ecosystems and services [79, 80]. The database values were aggregated into entries from 4 HDI brackets, the 8 biomes in which the ecosystems classifications sit - coral reefs, coastal systems, inland wetlands, lakes and rivers, tropical forest, temperate forest, woodland and shrubland, and grasslands, and into the three primary categories of services used in the ESVD – provisioning, regulating, and cultural services. The aggregated values had enough datapoints to draw samples and estimate total value of ecosystem services provided by 8 biomes per hectare (ha) per year (yr). See Annex A [4].

The output of module 104 provides ecosystem service values in international dollars for 8 biomes in country c in scenario s in the year t. Ecosystem service marginal values are used to determine damages to ecosystems from surface water run-off in the nitrogen emission costing model, and land-use changes in the land-use costing model. An extension of the blue water withdrawal costing model, which currently does not include the impact of future water scarcity on environmental flows and services outside of food provisioning, would also use ecosystem service marginal values.

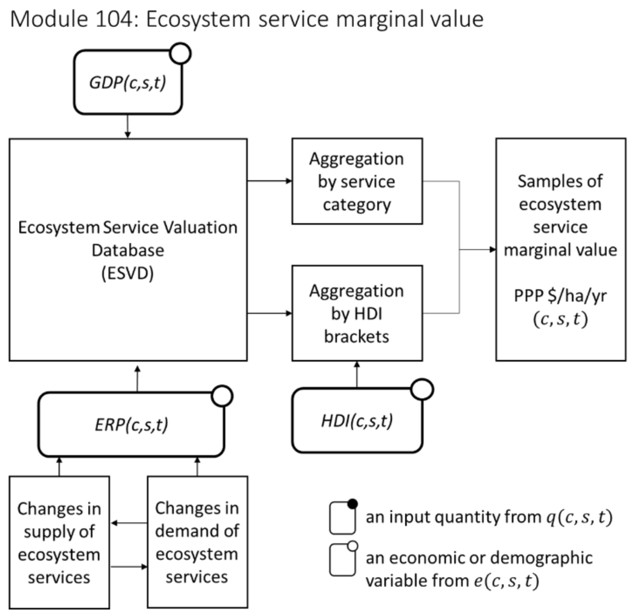

Figure 4: Aggregating values from the ecosystem services valuation database (ESVD) by HDI bracket, and by service category (provisioning, regulating, cultural) provides enough datapoints to estimate the distributions of ecosystem service value. The ESVD is in international dollars in 2020. Inflating the marginal values to a future time t in scenario s, for a country c, involves two adjustments to overall economic growth represented by GDP growth. Ecosystem services may become more or less valuable in the future due to reduced supply from environmental damage or increased supply from reversing environmental damage. Ecosystem services may also become more or less valuable depending on the utilisation of natural capital by the economy, including technological advances in the efficiency of using natural capital. The combined effect of future changes in supply and demand of ecosystem services is represented by a relative price factor (ERP) between general produced capital flows represented by GDP and natural capital flows represented by ecosystem services. Once adjusted values are aggregated by service category and HDI bracket, samples are obtained for a country c by using the distribution corresponding to the HDI bracket of country c at time t in scenario s.

The ESVD has ecosystem marginal values in international dollars in 2020, and we assume the marginal values in the ESVD relate to the value provided to an economy in 2020 by the ecosystem.

Inflating the marginal values to the value provided by an ecosystem at a future time t in scenario s, for a country c, involves adjustments to overall economic growth represented by GDP growth. The future supply and demand of ecosystem services is complex [81-83]. Ecosystem services may become more or less valuable in the future due to reduced supply from environmental damage or increased supply from reversing environmental damage [84]. Ecosystem services may also become more or less valuable depending on the utilisation of natural capital by the economy [85], including technological advances in the efficiency of using natural capital. SPIQ-FS damage estimates are based on consumption as income-equivalent welfare, therefore a relative price factor (ERP) for ecosystem services [86-88], with a base of 1 in the year 2020, is used to adjust GDP PPP growth.

Once adjusted values are aggregated by biome, service category, and HDI bracket, samples are obtained for a country c by using the distribution corresponding to the HDI bracket of country c at time t in scenario s.

1.3.5 Cost Model 01: marginal social costs of GHG emissions

The GHG costing model uses IGW-SCGHG simulations [19, 20, 89, 90]. The social cost of carbon simulations conducted by IGW-SCGHG used 5 scenarios and 3 discount rates to explore future uncertainty in economic activity. The IGW-SCGHG simulations provide, separately, samples of the social cost of a 1 metric ton emission of CH_4, CO_2 and N_2O gases [90-96] derived from Monte Carlo modelling for each IGW-SCGHG scenario, each discount rate, and for the emission occurring in the year 2020, 2030, 2040 or 2050. The IGW-SCGHG simulations can therefore be considered sets of samples of the marginal social cost, for each gas, indexed by IGW-SCGHG scenario, discount rate, and emission year.

The SPIQ-FS file requires that weights be specified to indicate the similarity of the build scenarios (s, t) "an emission of 1 metric ton of the specified gas at time t in the future s" to the IGW-SCGHG scenario, discount rate, and emission year. The weights are used to generate a joint sample of IGW-SCGHG scenario, discount rate, and emission year. For each element of the joint sample of IGW-SCGHG scenario, discount rate, and emission year a sample of the social cost of a GHG is then taken from the samples of SC corresponding to that IGW-SCGHG scenario, discount rate, and emission year. In this way, a sample set of SC-GHG values are obtained for the pair (s, t).

As explained in Annex A [1], the social costs of greenhouse emissions are global values and do not differ between countries since economic inequalities are not accounted [97, 98]. Social cost is taken as a lower estimate of damage cost, it represents the damage cost in an economy with optimal abatement. The output of the cost model 01 is a set of samples of the social cost of CH4, or CO2, or N2O, for each build scenario and emission time (s, t), that is, an emission of 1 metric ton of the specified gas at time t in the future s. As also explained in Annex A, CO2-equivalents are not used to convert emission in the separate gases to CO2 weight [96, 99, 100]. Doing so would distort the social costs of CH4 and N2O [20, 101]. Annex A explains joint sampling of the marginal social costs for use with emissions quantities [1].

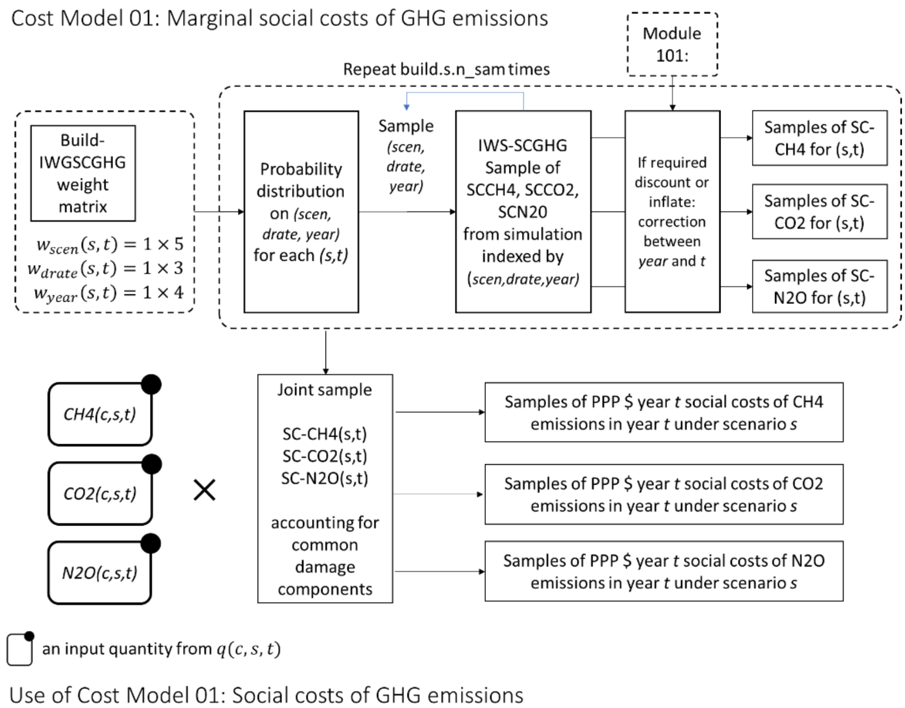

Figure 5: weights specified in a SPIQ-FS build file indicate how the IWG-SCGHG Monte-Carlo simulations of the social costs of CH4, CO2 and N2O can be used be used to obtain samples of the social costs of an emitted GHG in year t in the future scenario s.

1.3.6 Cost Model 02: marginal damage costs of blue water withdrawals

The blue water withdrawal costing model estimates future damages of water scarcity converted into international dollars (PPP) in year t.

Cost Model 02: Damage costs of blue water withdrawal

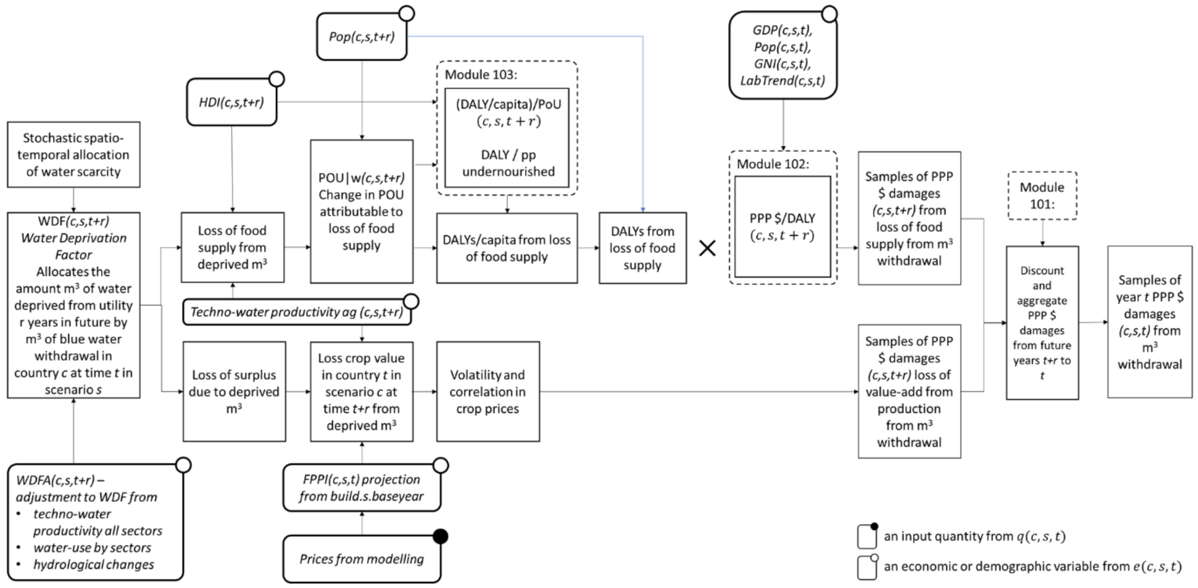

Figure 6: blue water withdrawal damages through the impacts of future water scarcity. Loss of food supply leads to malnutrition and productivity losses, and the impact of scarcity on sectors using water leads to loss of surplus.

The calculation assumes that water withdrawal in a water basin will impact the availability of water resources in that basin in future years after the withdrawal, either through depleting slow recharge water resources such as fossil water aquifers or through a reduction in the quantity of usable blue water such as increased salinity [102]. Future water economic users include industry, agriculture, drinking water and sanitation, and secondary services from ecosystems in the water basin [103, 104]. Future versions of the cost model aim to include costs of reduced environmental flows [105]. The amount of water deprived from economic users of the water in the basin at a future time $t + r$ due to blue water withdrawal in the basin at time t is called the water deprivation due to the blue water withdrawal.

Even if water markets operated in the future in the water basin [104], loss of economic value can occur from water deprivation through a cost increase or reduction in production of goods [103]. The model makes the simple assumption that the deprived water will concentrate in the agricultural sector [106, 107]. Water deprivation for agricultural use results in either malnutrition and productivity losses, or income losses [28].

The model for water deprivation is based on a lifecycle impact assessment method [108]. Though water deprivation is used as quantitative factor in [108] and is associated to water scarcity through a formula, it is not conceptually defined in [108]. The calculation of water deprivation in [108] is geospatially specific, being based on the water stress index of individual countries, but it is not temporally specific. It does not indicate what amount of water deprivation will occur when in the future. The default SPIQ-FS water cost model assumes that the calculation of water deprivation of [108] is the total water deprivation due to the blue water withdrawal, and allocates portions of the water withdrawal into the future using a Poisson process [109]. The Poisson rate depends on the water stress index of the country and groundwater versus surface water withdrawals. Countries with high water stress dependent on exploiting groundwater will experience water deprivation sooner than countries with low water stress and economies utilising mostly surface blue water.

There are very few, if any, modelled scenarios of global water scarcity out to 2100 in the literature [110]. Adapting them to replace the Poisson process allocation and the calculation of [108] is beyond the scope of version 0 of SPIQ-FS. The spatial-temporal allocation of water deprivation is one the components in the water model for whether damage costs are different between the build scenarios. Productivity gains in water-use by economic users in the country [111], whether the country shifts its economy to be less dependent on blue water natural capital [112], and the environmental conditions affecting hydrology in the basin [113], are the three main factors that may alter the water deprivation between the scenarios at time $t + r$ from the same amount of blue water withdrawal at time t. It would require complex coupled economic and environmental modelling to project global water deprivation out to 2100. To be pragmatic, to indicate the differences in scenario we alter the default water deprivation calculation by a multiplicative term $WDFA(c, s, t + r)$ which needs to be specified in the series of economic variables in Table 1. Trends for $WDFA(c, s,\cdot)$ where $t + r$ is greater than the maximum value for t are extended up to 2100 using Holt's linear trend method.

Water deprivation from agricultural use in year $t + r$ results in malnutrition and income effects. Ideally, an economic equilibrium would determine the balance between the two effects, the reduced domestic supply creates a shortfall in meeting domestic demand, which can result in higher prices for that supply and imports to meet the shortfall [114]. The shortfall in demand at equilibrium will result in malnutrition effects, and the net income losses from reduced supply but higher prices result in value loss to domestic agriculture (imports at higher prices may result in a gain to other countries). The calculation of [108] does not consider economic redistribution of shortfall demand. We assume the extreme poor bear the demand shortfall and therefore caloric loss from water deprivation. We assume income effects on non-extreme poor farmers are not sufficient to affect caloric intake - they suffer income losses equal to the reduction in production from the water deprivation. Extreme poor agricultural producers bear both demand shortfall and incomes losses from reduced production.

Shortfall in demand is translated to caloric loss in the domestic population, and thereby to an increase in the prevalence of undernourishment following the scheme of [108], the details are in Annex A [3]. Module 103 and module 102 are used to translate prevalence of undernourishment to health outcomes and associated costs of productivity in the year $t + r$. The discounting module then coverts the costs in $t + r$ to a comparable value to economies in year t. Module 103 describes how countries decrease in their vulnerability to undernourishment from loss of food production in the year $t + r$ compared to year t by either having higher real disposable incomes to reduce demand shortfall or having sufficient surplus of nourishment that the loss does not lead to undernourishment. Also, as countries increase in development, better healthcare leads to less disease outcomes from the same percentage of undernourished. The cost of a DALY from protein-energy malnutrition also changes as countries develop (Module 102). Roughly, the combination of Module 103 and Module 102 describes the changes in marginal labour productivity with undernourishment treated as an input.

The income loss from a deprived m^3 of blue water is based on a global spatial dataset of the monetary value of a m^3 of blue water to crops in 2020 [107]. The values in the dataset are projected to the year $t + r$ by considering country specific improvements in water efficiency and changes in farm-gate prices. Improvements in agricultural water efficiency from technology [115] are included by multiplying values in the data set by the factor $WPAA(c, s, t + r)$ below. Change in farm-gate prices relative to costs is incorporated by a Food Producer Price Index (FPPI) projection of country c in scenario s at time t with value 1 in the base year 2020. FPPI is the increase or decrease in farm gate prices relative to costs averaged across commodities [116]. FPPI needs to be specified in the series of economic variables in Table 1. Change in incomes from future trends in agricultural prices are included by multiplying values in the data set by $FPPI(c, s, t + r)$.

Water productivity improvements at same cost for all sectors is one of the considerations in the factor $WDFA$ [111]. However, the specific water productivity of the agricultural sector can mitigate the agricultural production losses from the water deprivation [115]. Since both productivity loss and income damages result from a change in agricultural production, a specific water productivity agricultural-sector adjustment is applied for country c in scenario s at time t, $WPAA(c, s, t + r)$, to reduce the effective water deprivation. $WPAA(c, s, t + r)$ needs to be specified in the series of economic variables in Table 1. $WPAA(c, s, t + r)$ is a proportional index estimating increases in volume of food supply (as a proxy for both caloric and value increase) from same water supply and same real costs of production. The baseline is 1 in 2020.

1.3.7 Cost Model 03: marginal damage costs of nitrogen emissions to air and surface waters

The nitrogen emissions costing model version 0 estimates damages in international dollars (PPP) in year t from volatilization of NH3 (ammonia) and NOx (nitrous oxides) to air [27], and run-off of reactive nitrogen into surface waters, predominately soluble NO3- (nitrate) [117]. Marginal costs for leaching of nitrate into subsoils and deep water sources [118, 119] are included in the cost model, but these costs in both marginal cost and total cost from quantity terms are generally less than the run-off to surface waters [120]. Ammonia is also the predominate cost of volatilized nitrogen from direct land-use activities, with NOx associated to transport and energy used in the production and consumption of food [121-125]. Emission of NOx is also more regulated than emission of NH3 [126, 127]. Nitrogen emissions are almost exclusively through production, with a minor part from food waste [128].

Due to the heterogeneity of manure treatment methods, the application of fertilizers, and climatic and soil conditions, it is difficult to base marginal costing on the quantities of application of synthetic fertilizer or head of livestock per acre [129]. The user of a SPIQ-FS dataset is required to calculate the four types of emissions (NH3 to air, NOx to air, Nr to surface water, Nr to deep waters). The nitrogen costing models does not include marginal N2O damage costs from primary or secondary emission [130], as they are included in the GHG costing model.

The damage costs from volatilization concentrate on human health effects, but also contribute to crop losses through terrestrial acidification and ozone production [121]. Additional surface water emission quantities from primary air emissions occur through deposition [117]. The damage costs from surface water run-off come from impact on ecosystem services downstream [117], with catchment specific percentages of nitrogen accumulating in terrestrial ecosystems fed by the water sources and then reaching coastal ecosystems [131, 132]. Acidification and eutrophication are the primary drivers of ecosystem impacts [133-135]. Eutrophication and some effects of acidification are consequences of biodiversity loss [136, 137]. Accumulated nitrogen from run-off can undergo secondary emission to air of NH3, NOx and N2O, [117]. The process of deposition and secondary emission from primary air and surface water emissions is called the nitrogen cascade [121].

Interactions between the global nitrogen, carbon, and methane cycles [117, 138, 139] are not fully represented by the separation of costing models. While excess nitrogen is responsible for biodiversity loss [140, 141] it increases sequestration through growth of biomass [138], so the effect on ecosystem services can be mixed. This interaction is not modelled directly, but factors into the correlation between nitrogen and CO2 marginal costs within SPIQ-FS.

Unlike the marginal value of water to crop production, presently there are no global spatial datasets of marginal loss to ecosystems services from exposure to excess soluble nitrogen, or marginal losses to human productivity from spatially specific emission of ammonia.

The most developed modelling of the air and surface water pathways has been done for the US [142], the EU nitrogen assessment [143, 144], and to an increasing degree in China [145, 146]. The most comprehensive study on marginal costs was conducted in the EU nitrogen assessment [147]. The developed modelling was used as the basis for transfer of the EU marginal costs, with the caveats mentioned in Annex A [2].

The human health modelling is most advanced, with high- and low-resolution chemical transport models available to model the exposure of human populations to sources of emissions [148-150]. The modelling calculates attributable DALYs by intersecting population densities with the contribution of ammonium particles to PM2.5 pollution. The SPIQ-FS model uses value transfer of a detailed county-level resolution of attributable DALYS from United States NH3 and NOx air pollution [151]. The United States has over 3000 counties. Transfer parameters for marginal cost included population density, temperature, NOx emissions, SOx emissions, and NH3 emissions [151, 152]. SOx and NOx emissions appear for several reasons, because most NH3 human health damage factors through the formation of ammonium compounds which require NOx and SOx to be present in the atmosphere [121], and NOx is also a proxy for economic activity due to its production by transport and energy sectors. DALYs are costed as productivity losses using module 102. NH3 and NOx human damage costs are strongly correlated, and this correlation was estimated from the sample set of 3000 counties and is applied in the SPIQ-FS uncertainty modelling.

Ozone costs from NOx emissions are transferred using FAO farm-gate cereal prices [117, 146, 153]. Transfer of the marginal costs of reactive nitrogen in surface waters is based upon the proportional transport of nitrogen to inland and coastal waterways using a global spatial dataset [119]. The relative value of ecosystem services in inland or coastal is used to value transfer based on a constant proportion between effective hectares of lost ecosystem services and emissions to surface waters. See Annex A [2]. Value of ecosystem services are provided by module 104. Costs from secondary emission in the surface water cascade is contained inside the calculation of the EU nitrogen assessment marginal values but cannot be adjusted to countries external to the EU without redoing the model of the EU nitrogen assessment.

The marginal costs of deposition on land are transferred using the same method based on proportion of deposition retained on land and relative value of ecosystem services from terrestrial ecosystems (tropical forests, temperate forests, woodland & shrubland, and grass & range-land) [136, 137, 154].

The effects of nitrogen pollution on waterways and ecosystem occur relatively quickly [155], so discounting is not used in the costing model for ecosystem effects. A perpetuating loss of services from a permanent alteration of ecosystems would be an additional costing component to future modelling. Time displacement between exposure to particulate matter and respiratory disease burden is assumed to be 10 years [120]. There is a considerable time lag between the onset of leaching and the nitrogen in deep water causing effects as nitrate in drinking water [155, 156]. Discounting is applied to this time lag.

Annex C

Cost Model 03: Damage costs of nitrogen emissions

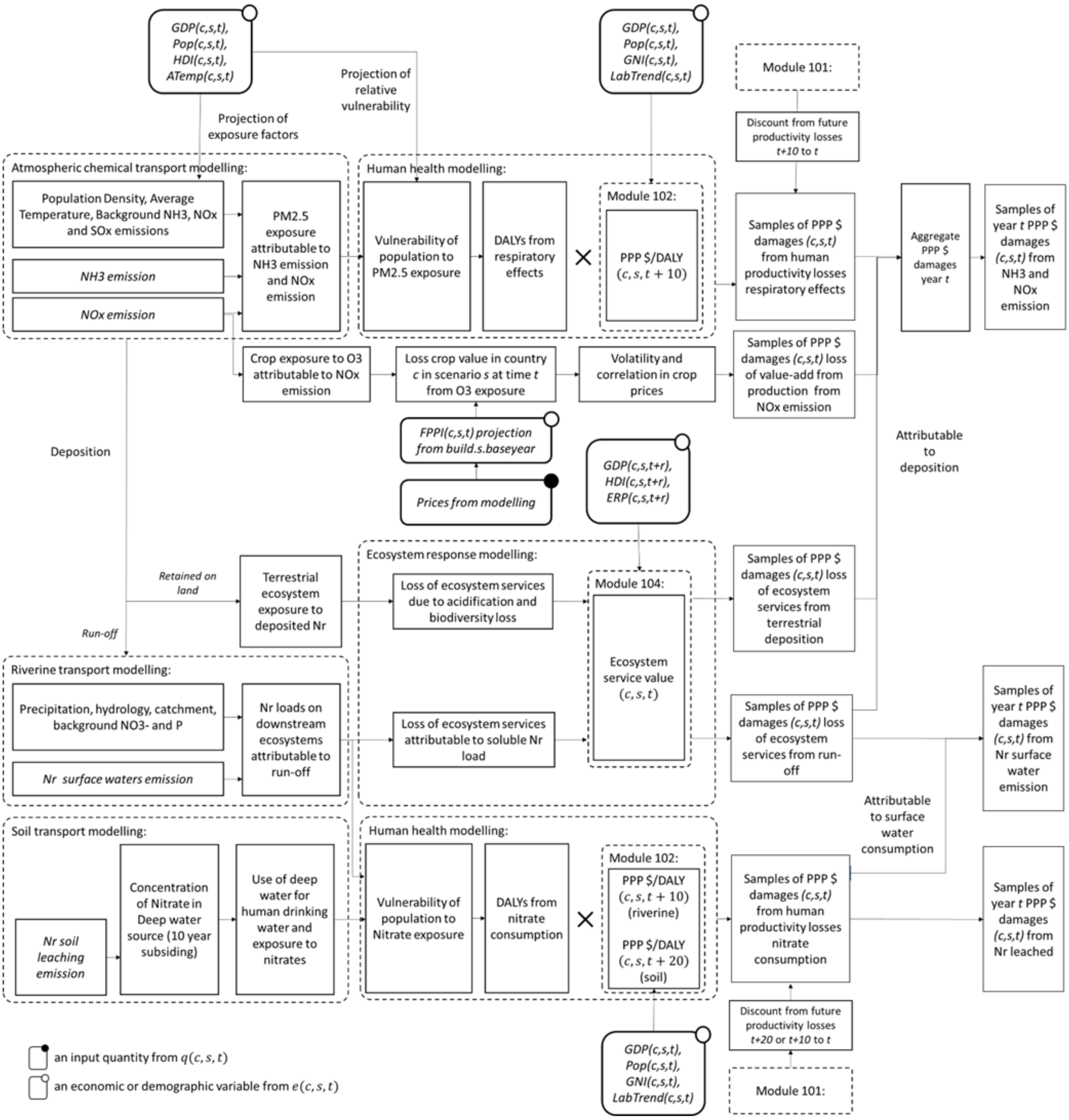

Figure 7: nitrogen emission damages through effects on human health and losses of ecosystem services. NH3 and NOx emissions to air lead to attributable PM2.5 exposure in downwind human populations. Riverine transport of Nr run-off from fields due to human application and deposition of emissions to air leads to, predominately, loss of ecosystem services through acidification, eutrophication, and biodiversity loss. Losses to crop production from O3 exposure due to NOx emission, and human health damage from exposure to nitrate in drinking water are, globally, lesser pathways to damages.

The SPIQ-FS nitrogen costing model version 0 is based on parametric value transfer with uncertainty. The transfer parameters allow costs to be projected temporally as well as transferred spatially.

Human health marginal damage costs from air emissions of NH3 and NOx are adjusted to a future time by changes to discount rate from module 101, temporal changes in productivity loss due to death or disability, and parametric adjustment of relative exposure factors. Parameters projected for exposure include Population, and GDP, ATemp, [151]. To project total NH3, NOx and SOx emissions, a vector autoregression model including NH3, NOx, SOx, GDP, Population and HDI was used. Using the GDP, Population, HDI and ATemp projections in the trained model resulted in NH3, NOx, SOx projections. The correlation between NH3 and NOx health damages was assumed too persistent unchanged. The projection of only exposure may omit future mitigation of PM2.5 health effects, including increased use masks or filtration in human living spaces, and improvements in population general health due to development [157]. Over 90% of the global burden or respiratory disease is estimate to occur in low and middle income countries despite developed countries have similar prevalence [158], indicating increased vulnerability as well as exposure at lower levels of development. Historical datasets of national DALYs due to respiratory disease (COPD) and PM2.5 exposure were available from the WHO [159] (https://www.who.int/data/gho/data/themes/mortality-and-global-health-estimates/global-health-estimates-leading-causes-of-dalys) and OECD (https://stats.oecd.org/Index.aspx?DataSetCode=EXP_PM2_5), respectively, and were used to transfer and project forward the relative effect of HDI for vulnerability to respiratory disease.

Ecosystem damage costs from deposition and surface water primary emissions are adjusted similarly by considering marginal changes in exposure and value loss. See Annex A [2]. Changes in the value of ecosystem services is projected within Module 104. While we have historical data that can be used to understand change in marginal changes in human productivity losses to PM2.5 exposure over time due to factors such as HDI, there are no global data sets to understand how the response of ecosystem services to the same load of nitrogen change over time across the categorical and spatial distribution of ecosystems. General environmental degradation due to climate change might exacerbate the value loss from the same exposure of nitrogen load, and accumulated nitrogen in the environmental [156] may also increase the damage to ecosystem function from the same load. In the absence of estimates of marginal changes in ecosystem productivity with nitrogen loads as inputs, we keep the effective loss of hectares of ecosystem services as a function of nitrogen loads constant over time. Damage from acidification of terrestrial ecosystems due to deposition of reactive nitrogen on land is treated similarly.

Nitrogen damage costs are spatially specific and transfers in the above costing model are based upon national averaging [160]. Temporal projections omit changes in the intranational distribution of populations, emission sites, and ecosystems. The projection also omits distributional and volumetric changes in nitrogen cascades due to continued emissions and environmental changes. As an example, saturation of nitrogen pools may increase the relative amounts of excess nitrogen in downstream ecosystem per unit of primary emission.

Ozone costs from NOx emissions were temporally projected using FPPI, which inflates 2020 FAO farm-gate cereal prices. This may omit mitigation effects in agricultural production, such as O3 resistant crops [161], or underestimate losses from increases in yield in exposed cropland (including changes in the distribution of cropland and crop types [162]).

Nitrate in drinking water due to leaching has relatively small marginal costs compared to the other nitrogen emission [120]. Outside of changes to discount rate from module 101 and the temporal changes in productivity loss due to death or disability, leaching marginal damage costs are not adjusted temporally for SPIQ-FS version 1. This may omit effects of organic and inorganic nitrogen saturation in soils from continued synthetic fertiliser use and livestock land-use. Neither improved nitrate filtration, nor increased reliance on groundwater drinking sources, in the future were considered.

1.3.8 Cost Model 04: marginal damage costs of land-use change

The land-use costing model estimates the value change in ecosystem services from land-use change in international dollars (PPP) in year t. The marginal value of ecosystem services in the units of ha/yr is obtained from the common module 104 and based on a statistical analysis of the ecosystem services valuation database (ESVD) [78, 163-166].

In important feature is the restoration of the services over time, or the adaptation of the economy to the services provided by the changed biome, so that the ecosystem services lost from the original biome can be projected forward in time for country c in year t under scenario s, [167]. This projection is difficult, because, like the water deprivation factor in cost model 02, it relies on specific consequential biophysical and economic modelling of the future scenarios, [81-83].

The projection of the persistence of the effects of the land-use change is used to aggregate and discount the damage costs from future years from the change affected in year t.

For most food and land-use studies will be conversion of cropland and pasture to forest and grassland (abandoned land), and conversion of grassland and forests to cropland and pasture (land-clearing) [168]. Studies suggest that biodiversity generally takes greater than 10 years to recover [169] with impacts still visible for up to 20 years [170] from agricultural land-clearing. Some changes, such as alteration of water retention and water filtrations services may effectively be permanent and require economic adaptation [171].

By default, SPIQ assumes a 20 year horizon for the effect of land-use changes with no additional adaptation of the economy to utilise the non-food or non-forest provision services provided by the new biome outside of that described by the social discount rate. This default setting allows the derived marginal damage costs for land use to be used in a modelling exercise where both land conversions to cropland and pasture, and future conversions of cropland and pasture back to grasslands or forest, are counted.

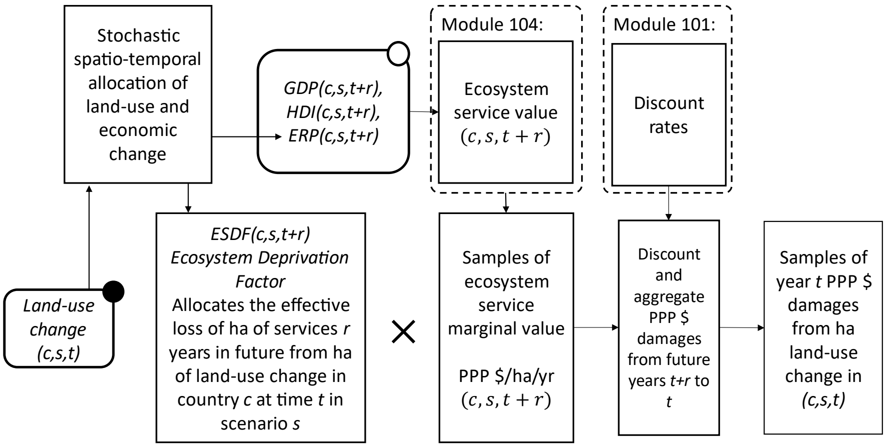

Figure 8: land-use change damages from effective loss of ha of ecosystem services. Module 104 provides estimates of the ecosystem service loss per ha for a future year. A modelling process needs to indicate the number of future years, and the degree of loss in those years, due to the ha of land-use change in country c in year t in scenario s. The land-use change is from one biome to another within the 8 biomes costed, or to a biome considered to provide no ecosystem services to be counted into the damage costing. The amount of change in future year is multiplied against the difference in value between the biomes, and then aggregated across the years of lost services with discounting applied.

1.3.9 Cost Model 05: marginal damage costs of undernourishment

The undernourishment costing model estimates damage to productivity from protein-energy malnutrition in international dollars (PPP) in year t.

The cost model pairs modules 102 and 103, to estimates of the FAO measure of the prevalence of undernourishment (PoU) in the quantities $q(c, s, t)$. A separate modelling process needs to estimate the future changes to PoU in country c in year t under scenario s.

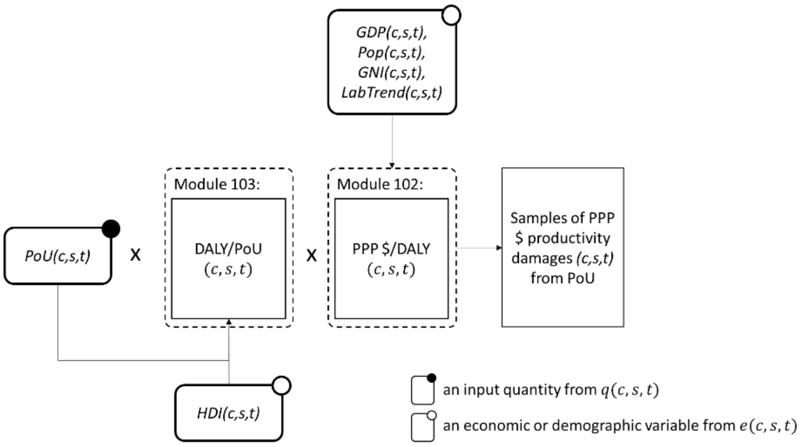

Figure 9: Module 103 estimates the DALYs from protein-energy malnutrition due to prevalence of undernourishment. HDI adds high explanatory power to a partial quadratic relationship between DALYs and PoU, and HDI trajectories in the set of economic and demographic projections associated to a scenario can be used to adjust the estimation of DALYs. The errors in the quadratic relationship are modelled as described in Annex A, allowing Module 103 to produce samples of DALYs due to a given level of PoU. The sampling depends on HDI. Module 102 estimates the productivity loss that results from the lost DALYs from protein-energy malnutrition. Module 102 is also adjusted by the economic and demographic projections associated to a scenario. Multiplying a given level of PoU against the outputs of module 103 and 102 provides samples of damage costs factoring through health outcomes for undernourishment.

There is a variant of the cost model that uses underweight (BMI < 18.5) in place of the FAO's measure of undernourishment. A separate modelling processes needs to estimate the future headcounts of the population below 18.5 for country c in year t under scenario s. The underweight variant of the cost model uses the underweight variant of common module 103, described in Section 1.3.3.

1.3.10 Cost Model 06: marginal damage costs of high body mass index

The cost model for high body mass index (BMI) uses modelled estimates of population BMI to estimate damage to productivity from health outcomes in international dollars (PPP) in year t.

The model has three parts (Figure 10). The first part uses the estimates of population BMI, the form of headcount within BMI intervals [72, 73] of the population of country c in year t under scenario s. The headcounts within BMI intervals are used to estimate the mean and standard deviation of BMI for exposure within the 30 subpopulations of the Institute for Health Metrics and Evaluation (IHME) Global Burden of Disease (GBD) high BMI model [22]. The GBD subpopulations partition the population into males and females for 15 different age brackets.

The mean and standard deviation estimates, for the GBD subpopulations, the exposure inputs for the IHME GBD high BMI model, which calculates population attributable fraction (PAF) [172, 173] of disease outcomes to high BMI. SPIQ-FS has replicated the IHME GBD high BMI model in the Python scientific programming language [174] as the second part of the costing model. Aggregating IHME GBD high BMI outputs estimates preventable disease and death due to high BMI in terms of DALYs. The DALY costing module (module 102) in SPIQ then converts DALYS to international dollars (PPP) in year t. The modelling is described in more detail in Annex A.

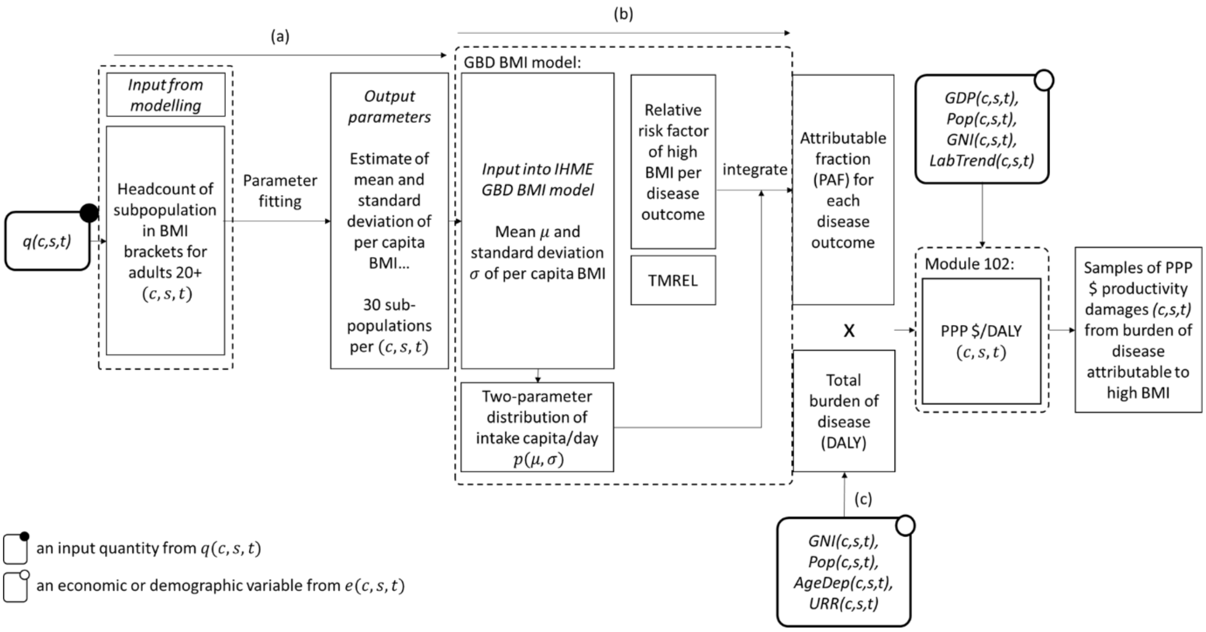

Figure 10: high body mass index (BMI) damages as productivity losses from disease outcomes. Temporal projection of the disease burden involves three components: (a) projecting the mean and standard deviation of the distribution of BMI in subpopulations in the country c in scenario s at time t; (b) the IMHE GBD BMI model maps the exposure to high BMI for subpopulations to the PAFs for disease outcomes, which is the fraction of the total disease burden (measured in DALYs) attributable to BMI > 25, and; (c) the total disease burden from noncommunicable diseases for subpopulations of the country c are predicted for the year t under the scenario s. Together (a) and (b) determine the attributable fractions from modelling output, which provides the change in DALYS for country c in year t under scenario s when the attributable fractions are multiplied by total disease burden and aggregated across the subpopulations. Module 2 is used to cost the DALY burden in terms of productivity losses. The calculation of BMI must come from modelling outcomes within q(c,s,t) and e(c,s,t), taking into account food supply, energy requirements, and physical activity. The current SPIQ model does not have an internal model to calculate the mean and standard deviation from food supply and economic and demographic variables.

Linking provided modelling of headcounts in BMI intervals for country c in year t under scenario s to the first two components of the costing model ((a) and (b) in Figure 10) calculates the PAFs which attribute total disease burden to high BMI. We assume the GBD relative risk curves remain constant, trends which could potentially alter the relative risk curves include advances or cost effectiveness in medical technology. We also assume that the GBD two-parameter family of distribution of BMI remains constant. Future trends could cause the shape of the distribution to change.

We make temporal adjustments to the costing model in module 102, described earlier, and to the total burden of disease ((c) in Figure 10). Projections of the total burden of disease for disease outcomes associated to BMI and dietary intake are the same and are described in the next section.

1.3.11 Cost Model 07: marginal damage costs of noncommunicable disease burden from dietary intake

The noncommunicable disease (NCD) burden from dietary intake costing model uses food supply quantities in the vector $q(c, s, t)$ and economic and demographic variables from $e(c, s, t)$ to estimate damage to productivity from the health effects of intake in international dollars (PPP) in year t.

The model has three parts (Figure 11). The first part uses FAO national food supply quantities and economic and demographic variables to estimate dietary intake distribution per capita for 30 subpopulations [175]. The subpopulations partition the population into males and females for 15 different age brackets. The per capita dietary intake distributions are the exposure inputs for the

Annex C

Institute for Health Metrics and Evaluation (IHME) Global Burden of Disease (GBD) NCD model [21], which calculates population attributable fraction (PAF) of disease outcomes to dietary intake. Dietary intake in the GBD NCD model is a mixture of diet components and nutrients [176]. SPIQ-FS has replicated in the Python scientific programming language [174] the IHME GBD NCD model as the second part of the costing model. Aggregating IHME GBD NCD outputs estimates preventable disease and death due to dietary intake in terms of DALYs. The DALY costing module (module 102) in SPIQ then converts DALYS to international dollars (PPP) in year t. The modelling is described in more detail in Annex A [5].

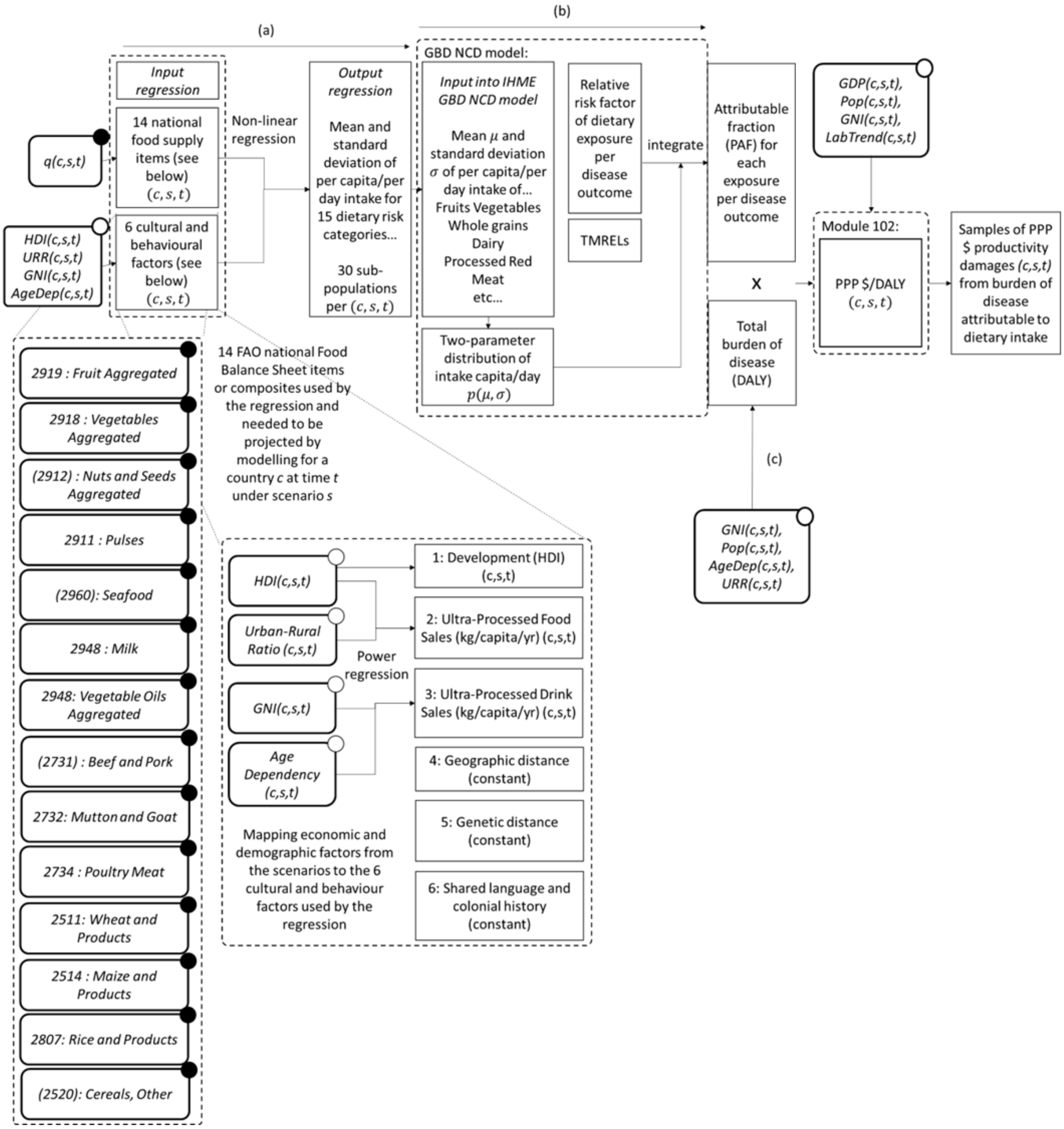

Figure 11: dietary intake damages as productivity losses from noncommunicable disease outcomes. Temporal projection of the disease burden involves three components: (a) 14 future food supply and 6 economic and demographic variables for the country c in scenario s at time t are mapped to the 15 dietary intake exposure categories for subpopulations in the IHME GBD model for non-communicable disease; (b) the IMHE GBD model maps 15 dietary intake exposure categories for subpopulations to the PAFs for disease outcomes, which is the fraction of the total disease burden (measured in DALYs) from noncommunicable diseases attributable to the dietary intake exposure, and; (c) the total disease burden from noncommunicable diseases for subpopulations of the country c are predicted for the year t under the scenario s. Together

(a) and (b) determine the attributable fractions from national food supply and economic and demographic changes, which provides the change in DALYS for country c in year t under scenario s when the attributable fractions are multiplied by total disease burden and aggregated across the subpopulations. Module 2 is used to cost the DALY burden in terms of productivity losses. The 14 food supply variables are based on FAO Food Balance Sheet (FBS) items with 4 digit code, or aggregates where the 4 digit item in brackets represents the dominant FBS item

We described the temporal components and inputs that can be used to adjust the costing model.

The non-linear regression using national food supply, and national economic and demographic variables, to predict dietary intake (the first part of cost model 07) require changes to 14 national food supply quantities to be encoded in $q(c, s, t)$. The national food supply variables used in the non-linear regression are FAO Food Balance Sheet (FBS) categories [177, 178], or aggregates of FAO FBS categories. Ten years of historical FAO FBS data in the categories from 2010-2019 were used to train and cross-validate the non-linear regression model [5]. Diets change in populations [179, 180] but evidence suggests they are relatively stable to train over a ten year window [181]. Non-linear regression [182, 183] far out-performed linear regression, showing that linear combination of national food supply components to estimate population dietary intake are inaccurate [184, 185] and do not account well for cooking processes [186], and food waste behaviour at the consumer level [187-189]. The non-linear regression also showed that clustering national dietary patterns was useful for reducing modelling error [190]. At present, the non-linear regression model cannot represent any structural changes – if new FBS categories (such as plant-based proteins) become significant in the future to dietary intake of whole grains, salt, polyunsaturated fats and trans-fats, the historically validated regression cannot reflect categorical changes. In this example, decrease in dairy and meat intake would be observed through increased in plant-based processed product supply in the historically trained regression, and effects from an increase in high processed foods – but not new effects from different categories of food products [191].

The non-linear regression uses 6 other variables that are designed to reflect cultural, behavioural, and economic differences that are relevant to differences in dietary intake [5, 180]. Three of the variables, representing geographic distances between countries [192], historical cultural factors [192], and genetic heritage [193], are assumed to be constant. Significant changes in these variables are assumed to occur over longer time frames than the period 2020-2050. The final three variables relate to income and nutrition transition. The variables are HDI which is a unitless index between 0 and 1, and ultra-processed food and drink sales (UPF and UPD [194]) in units of kg/capita/yr [195]. Development is expected to have a direct effect on the transformation of supply to intake through cooking and food waste behaviour, [187, 196, 197]. Basic functional regressions show strong explanation by an exponential relationship with UPF as a dependant variable of HDI and Urban-Rural Ratio (Figure 11) cross-validated by previous years [198, 199]. A similar regression shows moderate explanation by an exponential relationship with UPD as a dependant variable of GNI and Age Dependency (Figure 11) cross-validated by previous years [195, 200]. Over time the explanatory power of UPD by GNI has weakened. HDI, GNI, the Urban-Rural Ratio and Age-Dependency are correlated [201] national level statistics estimated by UNDP or World Bank. Including them in the economic and demographic factors $e(c, s, t)$ means that we can project forward in scenarios the cultural, behavioural, and economic differences relevant to differences in dietary intake, and take them into account when estimating PAFs for a country c in scenario s at time t.

The non-linear regression model, coupled to the replication of the IHME GBD NCD model within SPIQ, calculates PAFs within 30 subpopulations (characterised by gender and age) for the country c in the scenario s in year t.

The PAFs for disease outcomes (such as cardio-vascular disease, stomach cancer, etc.) need to be multiplied by the total number of DALYs attributed to the disease outcome in the 30 subpopulations in each country [172, 173]. Therefore, a separate modelling process (the third part of the costing model) needs to project forward the total DALY outcomes from NCDs for 30 subpopulations in each country. The IHME GBD now has a forecasting component, which projects forward the total DALYS from disease outcomes, however this forecasting process is not yet developed enough to be adaptable to different specifications of drivers and matched to build scenarios. Projections of regional or national total burden of disease exist based on current trends [202], but would require adjustment for alternative future scenarios. We do a simpler projection forward using population as one of the factors in $e(c, s, t)$ and a demographic profile that apportions the total population to the subpopulations. HDI and historical levels of the disease outcomes per capita in subpopulations are pooled across countries and times to project disease outcomes.

Combined, the temporal update to PAF calculations described, the projection of total burden of disease outcomes, and module 102 that projections forward costs of DALYS, are used to adjust the NCD from dietary intake costing model for a country c in the scenario s in year t.

2 References

1. Lord, S., *Estimations of marginal social costs for GHG emissions*, in *SPIQ-FS Dataset Version 0*. 2021, University of Oxford.
2. Lord, S., *Estimation of marginal damage costs from reactive nitrogen emissions to air, surface waters and groundwater*, in *SPIQ-FS Dataset Version 0*. 2021, University of Oxford.
3. Lord, S., *Estimation of marginal damage costs from water scarcity due to blue water withdrawal*, in *SPIQ-FS Dataset Version 0*. 2021, University of Oxford.
4. Lord, S., *Estimation of marginal damage costs for loss of ecosystem services from land-use change or ecosystem degradation*, in *SPIQ-FS Dataset Version 0*. 2021, University of Oxford.
5. Paulus, E. and S. Lord, *Estimation of marginal damage costs from consumption related health risks*, in *SPIQ-FS Dataset Version 0*. 2022, University of Oxford.
6. Barro, R.J., *Economic Growth in a Cross Section of Countries*.* The Quarterly Journal of Economics, 1991. **106**(2): p. 407-443.
7. Shapiro, A.C., *What does purchasing power parity mean?* Journal of International Money and Finance, 1983. **2**(3): p. 295-318.
8. Deb, S., *The Human Development Index and Its Methodological Refinements.* Social Change, 2015. **45**(1): p. 131-136.
9. Bank, W., *World development indicators 2007*. 2007: The World Bank.
10. Mathers, C.D. and D. Loncar, *Projections of Global Mortality and Burden of Disease from 2002 to 2030.* PLOS Medicine, 2006. **3**(11): p. e442.
11. Zivot, E. and J. Wang, *Vector Autoregressive Models for Multivariate Time Series*, in *Modeling Financial Time Series with S-Plus®*, E. Zivot and J. Wang, Editors. 2003, Springer New York: New York, NY. p. 369-413.
12. Laborde, D.L., Csilla; Martin, Will., *Poverty Impact of Food Price Shocks and Policies*, in *Policy Research Working Paper; No. 8724.* 2019, World Bank: Washington, DC.
13. Godfray, H.C.J., et al., *The future of the global food system.* Philosophical Transactions of the Royal Society of London B: Biological Sciences, 2010. **365**(1554): p. 2769-2777.
14. FABLE, *Pathways to Sustainable Land-Use and Food Systems. 2019 Report of the FABLE Consortium.* 2019, International Institute for Applied Systems Analysis (IIASA) and Sustainable Development Solutions Network (SDSN): Laxenburg and Paris.
15. FOLU, *Growing Better: Ten Critical Transitions to Transform Food and Land Use, The Global Consultation Report of the Food and Land Use Coalition.* 2019, Food and Land Use Coalition: New York.

16. Willett, W., et al., *Food in the Anthropocene: the EAT–Lancet Commission on healthy diets from sustainable food systems.* The Lancet, 2019. **393**(10170): p. 447-492.
17. van Asselt, M.B.A. and J. Rotmans, *Uncertainty in Integrated Assessment Modelling.* Climatic Change, 2002. **54**(1): p. 75-105.
18. Krysanova, V., F. Hattermann, and F. Wechsung, *Implications of complexity and uncertainty for integrated modelling and impact assessment in river basins.* Environmental Modelling & Software, 2007. **22**(5): p. 701-709.
19. IWGSCGG, *Technical Support Document: Technical Update of the Social Cost of Carbon for Regulatory Impact Analysis*. 2016, Interagency Working Group on Social Cost of Greenhouse Gases, United States Government: Washington DC.
20. IWGSCGG, *Technical Support Document: Technical Update of the Social Cost of Carbon, Methane and Nitrous Oxide Interim Estimates under Executive Order 13990*. 2021, Interagency Working Group on Social Cost of Greenhouse Gases, United States Government: Washington DC.
21. Afshin, A., et al., *Health effects of dietary risks in 195 countries, 1990–2017: a systematic analysis for the Global Burden of Disease Study 2017.* The Lancet, 2019. **393**(10184): p. 1958-1972.
22. Dai, H., et al., *The global burden of disease attributable to high body mass index in 195 countries and territories, 1990–2017: An analysis of the Global Burden of Disease Study.* PLOS Medicine, 2020. **17**(7): p. e1003198.
23. Christensen, P., K. Gillingham, and W. Nordhaus, *Uncertainty in forecasts of long-run economic growth.* Proceedings of the National Academy of Sciences, 2018. **115**(21): p. 5409.
24. Leimbach, M., et al., *Future growth patterns of world regions – A GDP scenario approach.* Global Environmental Change, 2017. **42**: p. 215-225.
25. Moore, M.A., et al., *"Just Give Me a Number!" Practical Values for the Social Discount Rate.* Journal of Policy Analysis and Management, 2004. **23**(4): p. 789-812.
26. Neumann, P.J., et al., *A Systematic Review of Cost-Effectiveness Studies Reporting Cost-per-DALY Averted.* PLOS ONE, 2016. **11**(12): p. e0168512.
27. de Vries, W., *Impacts of nitrogen emissions on ecosystems and human health: A mini review.* Current Opinion in Environmental Science & Health, 2021. **21**: p. 100249.
28. Fitton, N., et al., *The vulnerabilities of agricultural land and food production to future water scarcity.* Global Environmental Change, 2019. **58**: p. 101944.
29. Hsiang, S., et al., *Estimating economic damage from climate change in the United States.* Science, 2017. **356**(6345): p. 1362-1369.
30. Feng, Y., et al., *Review on pollution damage costs accounting.* Science of The Total Environment, 2021. **783**: p. 147074.
31. Yamaguchi, R. and S. Managi, *Backward- and Forward-looking Shadow Prices in Inclusive Wealth Accounting: An Example of Renewable Energy Capital.* Ecological Economics, 2019. **156**: p. 337-349.
32. Wu, D., et al., *Dynamics of pollutants' shadow price and its driving forces: An analysis on China's two major pollutants at provincial level.* Journal of Cleaner Production, 2021. **283**: p. 124625.
33. Tol, R.S.J., *Estimates of the Damage Costs of Climate Change, Part II. Dynamic Estimates.* Environmental and Resource Economics, 2002. **21**(2): p. 135-160.
34. Bertrand, T.J., *Shadow Pricing in Distorted Economies.* The American Economic Review, 1979. **69**(5): p. 902-914.
35. Chen, F. and Z. Chen, *Cost of economic growth: Air pollution and health expenditure.* Science of The Total Environment, 2021. **755**: p. 142543.
36. Wiebe, K., et al., *Scenario development and foresight analysis: exploring options to inform choices.* Annual Review of Environment and Resources, 2018. **43**.

37. Cantele, M., et al., *Equilibrium Modeling for Environmental Science: Exploring the Nexus of Economic Systems and Environmental Change.* Earth's Future, 2021. **9**(9): p. e2020EF001923.
38. van Tongeren, F., H. van Meijl, and Y. Surry, *Global models applied to agricultural and trade policies: a review and assessment.* Agricultural Economics, 2001. **26**(2): p. 149-172.
39. Bergman, L., *Chapter 24 CGE Modeling of Environmental Policy and Resource Management*, in *Handbook of Environmental Economics*, K.-G. Mäler and J.R. Vincent, Editors. 2005, Elsevier. p. 1273-1306.
40. Böhringer, C. and A. Löschel, *Computable general equilibrium models for sustainability impact assessment: Status quo and prospects.* Ecological Economics, 2006. **60**(1): p. 49-64.
41. Lyon, C., et al., *Climate change research and action must look beyond 2100.* Global Change Biology, 2022. **28**(2): p. 349-361.
42. Howarth, R.B., *Discounting and uncertainty in climate change policy analysis.* Land Economics, 2003. **79**(3): p. 369-381.
43. Weitzman, M.L., *A Review of the Stern Review on the Economics of Climate Change.* Journal of Economic Literature, 2007. **45**(3): p. 703-724.
44. Evans, D.J., *The Elasticity of Marginal Utility of Consumption: Estimates for 20 OECD Countries.* Fiscal Studies, 2005. **26**(2): p. 197-224.
45. Drupp, M.A., et al., *Discounting Disentangled.* American Economic Journal: Economic Policy, 2018. **10**(4): p. 109-34.
46. Lowe, J., *Intergenerational wealth transfers and social discounting: Supplementary Green Book guidance*. 2008, HM Treasury: London.
47. Roche, J., *Intergenerational equity and social discount rates: what have we learned over recent decades?* International Journal of Social Economics, 2016. **43**(12): p. 1539-1556.
48. Weitzman, M., *On Modeling and Interpreting the Economics of Catastrophic Climate Change.* The Review of Economics and Statistics, 2009. **91**(1): p. 1-19.
49. Gollier, C., *Pricing the planet's future : the economics of discounting in an uncertain world*. University Press Scholarship Online. 2017, Princeton: Princeton University Press.
50. Gollier, C., *Valuation of natural capital under uncertain substitutability.* Journal of Environmental Economics and Management, 2019. **94**: p. 54-66.
51. Gollier, C. and M.L. Weitzman, *How should the distant future be discounted when discount rates are uncertain?* Economics Letters, 2010. **107**(3): p. 350-353.
52. Arnesen, T. and E. Nord, *The value of DALY life: problems with ethics and validity of disability adjusted life years.* BMJ (Clinical research ed.), 1999. **319**(7222): p. 1423-1425.
53. Anand, S. and K. Hanson, *Disability-adjusted life years: a critical review.* Journal of Health Economics, 1997. **16**(6): p. 685-702.
54. Murray, C.J.L., et al., *GBD 2010: design, definitions, and metrics.* The Lancet, 2012. **380**(9859): p. 2063-2066.
55. Domingo, N.G.G., et al., *Air quality–related health damages of food.* Proceedings of the National Academy of Sciences, 2021. **118**(20): p. e2013637118.
56. Popkin, B.M., et al., *Measuring the full economic costs of diet, physical activity and obesity-related chronic diseases.* Obesity Reviews, 2006. **7**(3): p. 271-293.
57. Jardim, T.V., et al., *Cardiometabolic disease costs associated with suboptimal diet in the United States: A cost analysis based on a microsimulation model.* PLOS Medicine, 2019. **16**(12): p. e1002981.
58. Candari, C.J., J. Cylus, and E. Nolte, *European Observatory Health Policy Series*, in *Assessing the economic costs of unhealthy diets and low physical activity: An evidence review and proposed framework*. 2017, European Observatory on Health Systems and Policies, World Health Organization 2017: Copenhagen (Denmark).
59. Du, Y., et al., *Air particulate matter and cardiovascular disease: the epidemiological, biomedical and clinical evidence.* Journal of Thoracic Disease, 2015. **8**(1): p. E8-E19.

60. Bellou, V., et al., *Risk factors for type 2 diabetes mellitus: An exposure-wide umbrella review of meta-analyses.* PLOS ONE, 2018. **13**(3): p. e0194127.
61. Aykan, N.F., *Red Meat and Colorectal Cancer.* Oncol Rev, 2015. **9**(1): p. 288.
62. Liu, J., et al., *Evolving Patterns of Nutritional Deficiencies Burden in Low- and Middle-Income Countries: Findings from the 2019 Global Burden of Disease Study.* Nutrients, 2022. **14**(5).
63. Okunogbe, A., et al., *Economic impacts of overweight and obesity: current and future estimates for eight countries.* BMJ Global Health, 2021. **6**(10): p. e006351.
64. Rice, D.P., *Cost of illness studies: what is good about them?* Injury Prevention, 2000. **6**(3): p. 177.
65. Nugent, R., et al., *Economic effects of the double burden of malnutrition.* The Lancet, 2020. **395**(10218): p. 156-164.
66. Mitchell, R.J. and P. Bates, *Measuring health-related productivity loss.* Popul Health Manag, 2011. **14**(2): p. 93-8.
67. Springmann, M., *Valuation of the health and climate-change benefits of healthy diets*, in *FAO Agricultural Development Economics Working Papers. No 20-03*. 2020, Food and Agriculture Organization of the United Nations: Rome.
68. OECD, *Cross-country comparisons of labour productivity levels*. OECD Compendium of Productivity Indicators. 2021, Paris: OECD Publishing.
69. Gödecke, T., A.J. Stein, and M. Qaim, *The global burden of chronic and hidden hunger: Trends and determinants.* Global Food Security, 2018. **17**: p. 21-29.
70. Mathers, C.D., *History of global burden of disease assessment at the World Health Organization.* Archives of Public Health, 2020. **78**(1): p. 77.
71. Zhu, H. and R. Rohwer, *Bayesian regression filters and the issue of priors.* Neural Computing & Applications, 1996. **4**(3): p. 130-142.
72. Expert Panel on the Identification Treatment of Overweight Obesity in Adults, *Clinical guidelines on the identification, evaluation, and treatment of overweight and obesity in adults: the evidence report*. NIH Publications 98-4083. 1998, Bethesda, MD: National Institutes of Health, National Heart, Lung, and Blood Institute.
73. World Health Organization, *Obesity: preventing and managing the global epidemic*, in *WHO Technical Report Series 894*. 2000, World Health Organization: Geneva.
74. Katzmarzyk, P.T., C.L. Craig, and C. Bouchard, *Underweight, overweight and obesity: relationships with mortality in the 13-year follow-up of the Canada Fitness Survey.* Journal of Clinical Epidemiology, 2001. **54**(9): p. 916-920.
75. Kelly, S.J., et al., *Mental ill-health across the continuum of body mass index.* BMC Public Health, 2011. **11**: p. 765.
76. Costanza, R., et al., *The value of the world's ecosystem services and natural capital.* Nature, 1997. **387**(6630): p. 253-260.
77. Winkler, K., et al., *HILDA+ Global Land Use Change between 1960 and 2019*. 2020, PANGAEA.
78. de Groot, R., et al., *Global estimates of the value of ecosystems and their services in monetary units.* Ecosystem Services, 2012. **1**(1): p. 50-61.
79. Ring, I., et al., *Challenges in framing the economics of ecosystems and biodiversity: the TEEB initiative.* Current Opinion in Environmental Sustainability, 2010. **2**(1): p. 15-26.
80. Haines-Young, R. and M.B. Potschin-Young, *Revision of the Common International Classification for Ecosystem Services (CICES V5.1): A Policy Brief.* One Ecosystem, 2018. **3**: p. e27108.
81. Veerkamp, C.J., et al., *Future projections of biodiversity and ecosystem services in Europe with two integrated assessment models.* Regional Environmental Change, 2020. **20**(3): p. 103.
82. Rosa, I.M.D., et al., *Challenges in producing policy-relevant global scenarios of biodiversity and ecosystem services.* Global Ecology and Conservation, 2020. **22**: p. e00886.

83. Carpenter, S.R., E.M. Bennett, and G.D. Peterson, *Scenarios for Ecosystem Services: An Overview.* Ecology and Society, 2006. **11**(1).
84. Li, G., C. Fang, and S. Wang, *Exploring spatiotemporal changes in ecosystem-service values and hotspots in China.* Science of The Total Environment, 2016. **545-546**: p. 609-620.
85. Bryan, B.A., et al., *Land-use change impacts on ecosystem services value: Incorporating the scarcity effects of supply and demand dynamics.* Ecosystem Services, 2018. **32**: p. 144-157.
86. Heckenhahn, J. and M.A. Drupp, *Relative Price Changes of Ecosystem Services: Evidence from Germany*, in *CESifo Working Paper No. 9656*. 2022, CESifo: Munich.
87. Hoel, M. and T. Sterner, *Discounting and relative prices.* Climatic Change, 2007. **84**(3): p. 265-280.
88. Baumgärtner, S., et al., *Ramsey Discounting of Ecosystem Services.* Environmental and Resource Economics, 2015. **61**(2): p. 273-296.
89. Robert, E.K. and K.M. Bryan, *The U.S. Government's Social Cost of Carbon Estimates after their First Year: Pathways for Improvement.* Economics : the Open-Access, Open-Assessment e-Journal, 2011.
90. Nordhaus, W.D., *Revisiting the social cost of carbon.* Proceedings of the National Academy of Sciences of the United States of America, 2017. **114**(7): p. 1518.
91. Clarkson, R. and K. Deyes, *Estimating the social cost of carbon emissions*. Government Economic Service working paper. 2002, London: HM Treasury.
92. van den Bergh, J.C.J.M. and W.J.W. Botzen, *A lower bound to the social cost of CO2 emissions.* Nature Climate Change, 2014. **4**: p. 253.
93. Pindyck, R.S., *The social cost of carbon revisited.* Journal of Environmental Economics and Management, 2019. **94**: p. 140-160.
94. Tol, R.S.J., *The marginal damage costs of carbon dioxide emissions: an assessment of the uncertainties.* Energy Policy, 2005. **33**(16): p. 2064-2074.
95. Tol, R.S.J., *The Economic Impacts of Climate Change.* Review of Environmental Economics and Policy, 2018. **12**(1): p. 4-25.
96. Waldhoff, S., et al., *The Marginal Damage Costs of Different Greenhouse Gases: An Application of FUND.* Economics, 2014. **8**(1).
97. Ricke, K., et al., *Country-level social cost of carbon.* Nature Climate Change, 2018. **8**(10): p. 895-900.
98. Errickson, F.C., et al., *Equity is more important for the social cost of methane than climate uncertainty.* Nature, 2021. **592**(7855): p. 564-570.
99. Etminan, M., et al., *Radiative forcing of carbon dioxide, methane, and nitrous oxide: A significant revision of the methane radiative forcing.* Geophysical Research Letters, 2016. **43**(24): p. 12,614-12,623.
100. Lynch, J., et al., *Agriculture's Contribution to Climate Change and Role in Mitigation Is Distinct From Predominantly Fossil CO2-Emitting Sectors.* Frontiers in Sustainable Food Systems, 2021. **4**(300).
101. Marten, A.L. and S.C. Newbold, *Estimating the social cost of non-CO2 GHG emissions: Methane and nitrous oxide.* Energy Policy, 2012. **51**: p. 957-972.
102. van Vliet, M.T.H., et al., *Global water scarcity including surface water quality and expansions of clean water technologies.* Environmental Research Letters, 2021. **16**(2): p. 024020.
103. Henderson, J., et al., *Economic impacts of climate change on water resources in the coterminous United States.* Mitigation and Adaptation Strategies for Global Change, 2015. **20**(1): p. 135-157.
104. Koopman, J.F.L., et al., *The potential of water markets to allocate water between industry, agriculture, and public water utilities as an adaptation mechanism to climate change.* Mitigation and Adaptation Strategies for Global Change, 2017. **22**(2): p. 325-347.
105. Liu, X., et al., *Environmental flow requirements largely reshape global surface water scarcity assessment.* Environmental Research Letters, 2021. **16**(10): p. 104029.

106. Rosa, L., et al., *Global agricultural economic water scarcity.* Science Advances, 2020. **6**(18): p. eaaz6031.
107. D'Odorico, P., et al., *The global value of water in agriculture.* Proceedings of the National Academy of Sciences, 2020. **117**(36): p. 21985.
108. Pfister, S., A. Koehler, and S. Hellweg, *Assessing the Environmental Impacts of Freshwater Consumption in LCA.* Environmental Science & Technology, 2009. **43**(11): p. 4098-4104.
109. Li, Y., Y. Dong, and J. Qian, *Higher-order analysis of probabilistic long-term loss under nonstationary hazards.* Reliability Engineering & System Safety, 2020. **203**: p. 107092.
110. Dolan, F., et al., *Evaluating the economic impact of water scarcity in a changing world.* Nature Communications, 2021. **12**(1): p. 1915.
111. Kijne, J.W., R. Barker, and D.J. Molden, *Water Productivity in Agriculture: Limits and Opportunities for Improvement*. 2003, Wallingford, UK: CABI. 332.
112. Kong, Y., et al., *Decoupling economic growth from water consumption in the Yangtze River Economic Belt, China.* Ecological Indicators, 2021. **123**: p. 107344.
113. Clifton, C.F., et al., *Effects of climate change on hydrology and water resources in the Blue Mountains, Oregon, USA.* Climate Services, 2018. **10**: p. 9-19.
114. Motoshita, M., et al., *Consistent characterisation factors at midpoint and endpoint relevant to agricultural water scarcity arising from freshwater consumption.* The International Journal of Life Cycle Assessment, 2018. **23**(12): p. 2276-2287.
115. Molden, D., et al., *Improving agricultural water productivity: Between optimism and caution.* Agricultural Water Management, 2010. **97**(4): p. 528-535.
116. FAO, *Agriculture producer prices indices. 2015-2019.*, in *FAOSTAT Analytical Brief 26*. 2021, Food and Agricultural Organization of the United Nations: Rome.
117. Erisman, J.W., et al., *Consequences of human modification of the global nitrogen cycle.* Philosophical transactions of the Royal Society of London. Series B, Biological sciences, 2013. **368**(1621): p. 20130116-20130116.
118. Ascott, M.J., et al., *Global patterns of nitrate storage in the vadose zone.* Nature Communications, 2017. **8**(1): p. 1416.
119. Beusen, A.H.W., et al., *Coupling global models for hydrology and nutrient loading to simulate nitrogen and phosphorus retention in surface water – description of IMAGE–GNM and analysis of performance.* Geosci. Model Dev., 2015. **8**(12): p. 4045-4067.
120. van Grinsven, H.J.M., A. Rabl, and T.M. de Kok, *Estimation of incidence and social cost of colon cancer due to nitrate in drinking water in the EU: a tentative cost-benefit assessment.* Environmental health : a global access science source, 2010. **9**: p. 58-58.
121. Fowler, D., et al., *The global nitrogen cycle in the twenty-first century.* Philosophical Transactions of the Royal Society B: Biological Sciences, 2013. **368**(1621): p. 20130164.
122. Olivier, J.G.J., et al., *Global air emission inventories for anthropogenic sources of NOx, NH3 and N2O in 1990.* Environmental Pollution, 1998. **102**(1, Supplement 1): p. 135-148.
123. McDuffie, E.E., et al., *A global anthropogenic emission inventory of atmospheric pollutants from sector- and fuel-specific sources (1970–2017): an application of the Community Emissions Data System (CEDS).* Earth Syst. Sci. Data, 2020. **12**(4): p. 3413-3442.
124. Paulot, F., et al., *Ammonia emissions in the United States, European Union, and China derived by high-resolution inversion of ammonium wet deposition data: Interpretation with a new agricultural emissions inventory (MASAGE_NH3).* Journal of Geophysical Research: Atmospheres, 2014. **119**(7): p. 4343-4364.
125. Crippa, M., et al., *Gridded emissions of air pollutants for the period 1970–2012 within EDGAR v4.3.2.* Earth Syst. Sci. Data, 2018. **10**(4): p. 1987-2013.
126. Butraw, D. and S.J.F. Szambelan, *Emissions Trading Markets for SO2 and NOx*, in *Resources for the Future Discussion Paper No. 09-40*. 2009, Resources for the Future: Washington, DC.
127. Lu, X., et al., *The underappreciated role of agricultural soil nitrogen oxide emissions in ozone pollution regulation in North China.* Nature Communications, 2021. **12**(1): p. 5021.

128. Uwizeye, A., et al., *Nitrogen emissions along global livestock supply chains.* Nature Food, 2020. **1**(7): p. 437-446.
129. Dalgaard, T., et al., *Effects of farm heterogeneity and methods for upscaling on modelled nitrogen losses in agricultural landscapes.* Environ Pollut, 2011. **159**(11): p. 3183-92.
130. Galloway, J.N., et al., *Transformation of the Nitrogen Cycle: Recent Trends, Questions, and Potential Solutions.* Science, 2008. **320**(5878): p. 889.
131. Camargo, J.A. and Á. Alonso, *Ecological and toxicological effects of inorganic nitrogen pollution in aquatic ecosystems: A global assessment.* Environment International, 2006. **32**(6): p. 831-849.
132. Anthony, K.R.N., et al., *Ocean acidification causes bleaching and productivity loss in coral reef builders.* Proceedings of the National Academy of Sciences, 2008. **105**(45): p. 17442.
133. Zhu, L., et al., *Sources and Impacts of Atmospheric NH3: Current Understanding and Frontiers for Modeling, Measurements, and Remote Sensing in North America.* Current Pollution Reports, 2015. **1**(2): p. 95-116.
134. Sutton, M.A., et al., *Towards a climate-dependent paradigm of ammonia emission and deposition.* Philosophical Transactions of the Royal Society B: Biological Sciences, 2013. **368**(1621): p. 20130166.
135. Krupa, S.V., *Effects of atmospheric ammonia (NH3) on terrestrial vegetation: a review.* Environmental Pollution, 2003. **124**(2): p. 179-221.
136. Tian, D. and S. Niu, *A global analysis of soil acidification caused by nitrogen addition.* Environmental Research Letters, 2015. **10**(2): p. 024019.
137. Bowman, W.D., et al., *Negative impact of nitrogen deposition on soil buffering capacity.* Nature Geoscience, 2008. **1**(11): p. 767-770.
138. Pinder, R.W., et al., *Impacts of human alteration of the nitrogen cycle in the US on radiative forcing.* Biogeochemistry, 2013. **114**(1): p. 25-40.
139. Zhu, Q., et al., *Cropland acidification increases risk of yield losses and food insecurity in China.* Environmental Pollution, 2020. **256**: p. 113145.
140. Bobbink, R., et al., *Global assessment of nitrogen deposition effects on terrestrial plant diversity: a synthesis.* Ecological Applications, 2010. **20**(1): p. 30-59.
141. Stevens, C.J., T.I. David, and J. Storkey, *Atmospheric nitrogen deposition in terrestrial ecosystems: Its impact on plant communities and consequences across trophic levels.* Functional Ecology, 2018. **32**(7): p. 1757-1769.
142. Sobota, D.J., et al., *Cost of reactive nitrogen release from human activities to the environment in the United States.* Environmental Research Letters, 2015. **10**(2): p. 025006.
143. van Grinsven, H.J.M., et al., *Costs and Benefits of Nitrogen for Europe and Implications for Mitigation.* Environmental Science & Technology, 2013. **47**(8): p. 3571-3579.
144. Sutton, M.A., et al., *Too much of a good thing.* Nature, 2011. **472**(7342): p. 159-161.
145. Gu, B., et al., *Atmospheric Reactive Nitrogen in China: Sources, Recent Trends, and Damage Costs.* Environmental Science & Technology, 2012. **46**(17): p. 9420-9427.
146. Feng, Z., et al., *Economic losses due to ozone impacts on human health, forest productivity and crop yield across China.* Environment International, 2019. **131**: p. 104966.
147. *The European Nitrogen Assessment: Sources, Effects and Policy Perspectives*. 2011, Cambridge: Cambridge University Press.
148. Gilmore, E.A., et al., *An inter-comparison of the social costs of air quality from reduced-complexity models.* Environmental Research Letters, 2019. **14**(7): p. 074016.
149. Matthias, V., et al., *Modeling emissions for three-dimensional atmospheric chemistry transport models.* Journal of the Air & Waste Management Association, 2018. **68**(8): p. 763-800.
150. Dore, A.J., et al., *Evaluation of the performance of different atmospheric chemical transport models and inter-comparison of nitrogen and sulphur deposition estimates for the UK.* Atmospheric Environment, 2015. **119**: p. 131-143.

151. Heo, J., P.J. Adams, and H.O. Gao, *Reduced-form modeling of public health impacts of inorganic PM2.5 and precursor emissions.* Atmospheric Environment, 2016. **137**: p. 80-89.
152. Philip, S., et al., *Global Chemical Composition of Ambient Fine Particulate Matter for Exposure Assessment.* Environmental Science & Technology, 2014. **48**(22): p. 13060-13068.
153. Avnery, S., et al., *Global crop yield reductions due to surface ozone exposure: 2. Year 2030 potential crop production losses and economic damage under two scenarios of O3 pollution.* Atmospheric Environment, 2011. **45**(13): p. 2297-2309.
154. Hesterberg, R., et al., *Deposition of nitrogen-containing compounds to an extensively managed grassland in central Switzerland.* Environmental Pollution, 1996. **91**(1): p. 21-34.
155. Billen, G., J. Garnier, and L. Lassaletta, *The nitrogen cascade from agricultural soils to the sea: modelling nitrogen transfers at regional watershed and global scales.* Philosophical Transactions of the Royal Society B: Biological Sciences, 2013. **368**(1621): p. 20130123.
156. Bijay, S. and E. Craswell, *Fertilizers and nitrate pollution of surface and ground water: an increasingly pervasive global problem.* SN Applied Sciences, 2021. **3**(4): p. 518.
157. Guan, W.-J., et al., *Impact of air pollution on the burden of chronic respiratory diseases in China: time for urgent action.* The Lancet, 2016. **388**(10054): p. 1939-1951.
158. Safiri, S., et al., *Burden of chronic obstructive pulmonary disease and its attributable risk factors in 204 countries and territories, 1990-2019: results from the Global Burden of Disease Study 2019.* BMJ, 2022. **378**: p. e069679.
159. WHO, *WHO methods and data sources for global burden of disease estimates 2000-2019*, in *Global Health Estimates Technical Paper WHO/ DDI/DNA/GHE/2020.3*. 2020, World Health Organization: Geneva.
160. Keeler, B.L., et al., *The social costs of nitrogen.* Science Advances, 2016. **2**(10): p. e1600219.
161. Frei, M., *Breeding of ozone resistant rice: Relevance, approaches and challenges.* Environmental Pollution, 2015. **197**: p. 144-155.
162. Bren d'Amour, C., et al., *Future urban land expansion and implications for global croplands.* Proceedings of the National Academy of Sciences, 2017. **114**(34): p. 8939-8944.
163. Costanza, R., et al., *Changes in the global value of ecosystem services.* Global Environmental Change, 2014. **26**: p. 152-158.
164. Magalhães Filho, L., et al., *A Global Meta-Analysis for Estimating Local Ecosystem Service Value Functions.* Environments, 2021. **8**(8).
165. Plummer, M.L., *Assessing benefit transfer for the valuation of ecosystem services.* Frontiers in Ecology and the Environment, 2009. **7**(1): p. 38-45.
166. Schmidt, S., A.M. Manceur, and R. Seppelt, *Uncertainty of Monetary Valued Ecosystem Services – Value Transfer Functions for Global Mapping.* PLOS ONE, 2016. **11**(3): p. e0148524.
167. Renard, D., M. Rhemtulla Jeanine, and M. Bennett Elena, *Historical dynamics in ecosystem service bundles.* Proceedings of the National Academy of Sciences, 2015. **112**(43): p. 13411-13416.
168. Winkler, K., et al., *Global land use changes are four times greater than previously estimated.* Nature Communications, 2021. **12**(1): p. 2501.
169. Jung, M., P. Rowhani, and J.P.W. Scharlemann, *Impacts of past abrupt land change on local biodiversity globally.* Nature Communications, 2019. **10**(1): p. 5474.
170. Le Provost, G., et al., *Land-use history impacts functional diversity across multiple trophic groups.* Proceedings of the National Academy of Sciences, 2020. **117**(3): p. 1573-1579.
171. Gomes, L.C., et al., *Land use change drives the spatio-temporal variation of ecosystem services and their interactions along an altitudinal gradient in Brazil.* Landscape Ecology, 2020. **35**(7): p. 1571-1586.
172. Vos, T., et al., *Global burden of 369 diseases and injuries in 204 countries and territories, 1990–2019: a systematic analysis for the Global Burden of Disease Study 2019.* The Lancet, 2020. **396**(10258): p. 1204-1222.

173. Walter, S.D., *The Estimation and Interpretation of Attributable Risk in Health Research.* Biometrics, 1976. **32**(4): p. 829-849.
174. Python Software Foundation, *Python Language Reference, version 2.7*.
175. Gebremedhin, S. and T. Bekele, *Evaluating the African food supply against the nutrient intake goals set for preventing diet-related non-communicable diseases: 1990 to 2017 trend analysis.* PLOS ONE, 2021. **16**(1): p. e0245241.
176. Hu, F.B., *Dietary pattern analysis: a new direction in nutritional epidemiology.* Curr Opin Lipidol, 2002. **13**(1): p. 3-9.
177. FAO, *FAOSTAT Food Supply Balance Sheets*. 2022, Food and Agriculture Organization of the United Nations.
178. Thar, C.M., et al., *A review of the uses and reliability of food balance sheets in health research.* Nutr Rev, 2020. **78**(12): p. 989-1000.
179. Pradhan, P., D.E. Reusser, and J.P. Kropp, *Embodied Greenhouse Gas Emissions in Diets.* PLOS ONE, 2013. **8**(5): p. e62228.
180. Kearney, J., *Food consumption trends and drivers.* Philos Trans R Soc Lond B Biol Sci, 2010. **365**(1554): p. 2793-807.
181. Kimokoti, R.W., et al., *Stability of the Framingham Nutritional Risk Score and its component nutrients over 8 years: the Framingham Nutrition Studies.* European Journal of Clinical Nutrition, 2012. **66**(3): p. 336-344.
182. Fan, J., J. Lv, and L. Qi, *Sparse High-Dimensional Models in Economics.* Annual Review of Economics, 2011. **3**(1): p. 291-317.
183. Athey, S. and G.W. Imbens, *Machine Learning Methods That Economists Should Know About.* Annual Review of Economics, 2019. **11**(1): p. 685-725.
184. Del Gobbo, L.C., et al., *Assessing global dietary habits: a comparison of national estimates from the FAO and the Global Dietary Database.* Am J Clin Nutr, 2015. **101**(5): p. 1038-46.
185. Rodríguez-Artalejo, F., et al., *Food supply versus household survey data: nutrient consumption trends for Spain, 1958-1988.* Eur J Epidemiol, 1996. **12**(4): p. 367-71.
186. Murphy, E.W., P.E. Criner, and B.C. Gray, *Comparisons of methods for calculating retention of nutrients in cooked foods.* J Agric Food Chem, 1975. **23**(6): p. 1153-7.
187. Verma, M.v.d.B., et al., *Consumers discard a lot more food than widely believed: Estimates of global food waste using an energy gap approach and affluence elasticity of food waste.* PLOS ONE, 2020. **15**(2): p. e0228369.
188. Dou, Z. and J.D. Toth, *Global primary data on consumer food waste: Rate and characteristics – A review.* Resources, Conservation and Recycling, 2021. **168**: p. 105332.
189. Schanes, K., K. Dobernig, and B. Gözet, *Food waste matters - A systematic review of household food waste practices and their policy implications.* Journal of Cleaner Production, 2018. **182**: p. 978-991.
190. Millen, B.A., et al., *Validation of a Dietary Pattern Approach for Evaluating Nutritional Risk: The Framingham Nutrition Studies.* Journal of the American Dietetic Association, 2001. **101**(2): p. 187-194.
191. Humpenöder, F., et al., *Projected environmental benefits of replacing beef with microbial protein.* Nature, 2022. **605**(7908): p. 90-96.
192. Head, K. and T. Mayer, *Chapter 3 - Gravity Equations: Workhorse,Toolkit, and Cookbook*, in *Handbook of International Economics*, G. Gopinath, E. Helpman, and K. Rogoff, Editors. 2014, Elsevier. p. 131-195.
193. Spolaore, E. and R. Wacziarg, *Ancestry and development: New evidence.* Journal of Applied Econometrics, 2018. **33**(5): p. 748-762.
194. Marino, M., et al., *A Systematic Review of Worldwide Consumption of Ultra-Processed Foods: Findings and Criticisms.* Nutrients, 2021. **13**(8).
195. Vandevijvere, S., et al., *Global trends in ultraprocessed food and drink product sales and their association with adult body mass index trajectories.* Obesity Reviews, 2019. **20**(S2): p. 10-19.

196. Chalak, A., et al., *The global economic and regulatory determinants of household food waste generation: A cross-country analysis.* Waste Management, 2016. **48**: p. 418-422.
197. Ishangulyyev, R., S. Kim, and S.H. Lee, *Understanding Food Loss and Waste-Why Are We Losing and Wasting Food?* Foods, 2019. **8**(8).
198. Reardon, T., et al., *The processed food revolution in African food systems and the double burden of malnutrition.* Global Food Security, 2021. **28**: p. 100466.
199. Baker, P., et al., *Ultra-processed foods and the nutrition transition: Global, regional and national trends, food systems transformations and political economy drivers.* Obes Rev, 2020. **21**(12): p. e13126.
200. Monteiro, C.A., et al., *Ultra-processed products are becoming dominant in the global food system.* Obesity Reviews, 2013. **14**(S2): p. 21-28.
201. Tripathi, S., *How does urbanization affect the human development index? A cross-country analysis.* Asia-Pacific Journal of Regional Science, 2021. **5**(3): p. 1053-1080.
202. Sleeman, K.E., et al., *The escalating global burden of serious health-related suffering: projections to 2060 by world regions, age groups, and health conditions.* The Lancet Global Health, 2019. **7**(7): p. e883-e892.